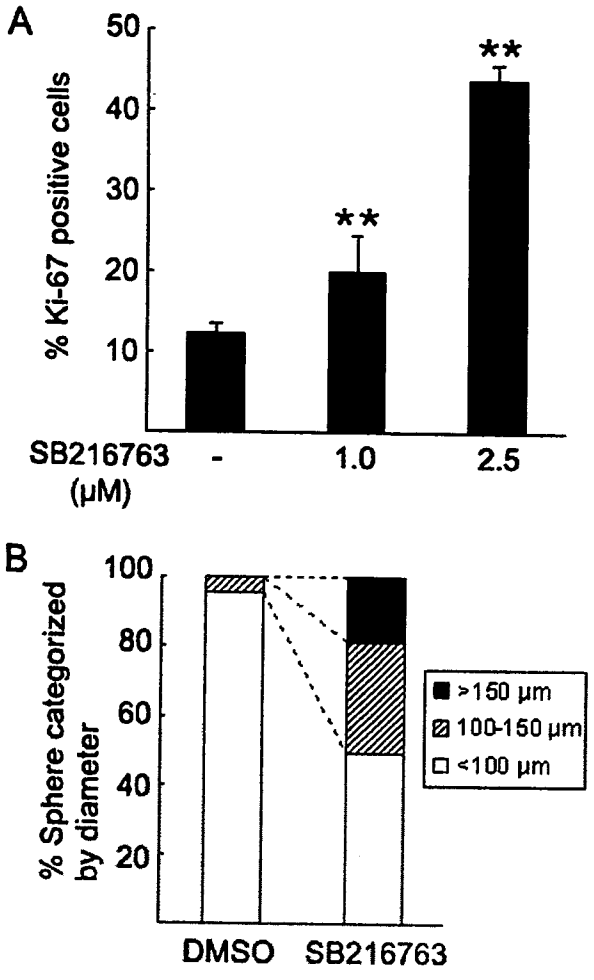

Figure 6. Increase in cell proliferation induced by SB216763 (a GSK3 inhibitor). **(A):** The percentage of Ki-67–positive cells was examined over the same time course described in the legend for Figure 2. The primary spheres were triturated and cultured in the adherent condition with SB216763 for 48 hours. Addition of 2.5 μM SB216763 increases the Ki-67-positive cells to 45% of the total cells. The results are the means ± standard deviations of three replicates. **p &λτ; 0.01 χομπαρεδ ωιτη χοντρολ χυλτυρεσ. B) Τηε περχενταγεσ οφ τηε σπηερεσ ωερε χατεγοριζεδ βψ τηειρ διαμετερ ασ δεσχριβεδ ιν τηε λεγενδ φορ Φιγυρε 3. A λαργε προπορτιον οφ σπηερεσ ιν τηε χυλτυρε χονταινινγ 2.5 μM SB216763 have diameters greater than 100 μm, whereas most spheres in the dimethylsulfoxide (DMSO)-treated control culture have diameters of 100 μm or less. The results are representative of three replicate experiments. The percentages of sphere-forming cells with DMSO and SB216763 were 0.098% ± 0.02% and 0.10% ± 0.01%, respectively.

AQ: 6

inhibitory molecule that is widely used to specifically interfere with signaling downstream of the FGF receptor (FGFR) [28]. Addition of FGF2 at 10 ng/ml to sphere-derived cell cultures increased the Ki-67–positive cells by threefold, and this activity was reduced to the control level by 6.0 μg/ml SU5402 (Fig. 7A). SU5402 decreased Ki-67–positive cells even in the absence of exogenous FGF2, supporting that endogenous FGF2 signaling was involved in the proliferation of retinal stem cells.

F7

We then added the FGFR inhibitor (SU5402) or FGF2 to the sphere-derived cell cultures in the presence of the GSK3 inhibitor (SB216763) and assessed the number of Ki-67–positive cells. Under all of the above conditions, there was no difference in the cell death estimated by immunocytochemical detection of activated caspase-3 (data not shown). Interestingly, the FGFR inhibitor attenuated the effect of the GSK3 inhibitor on cell proliferation and reduced the number of Ki-67–positive cells from 44%–18% (Fig. 7B). In contrast, exogenous FGF2 enhanced the proliferative effect of the GSK3 inhibitor and increased the Ki-67–positive cells to nearly 80% of the total cells, suggesting that there is an intense cooperative effect of FGF2 and Wnt signaling on cell proliferation of adult retinal sphere-derived cells.

Discussion

In the present study, we showed that Wnt3a increased the number of secondary spheres (promoting self-renewal) and that the expanded cells in the presence of Wnt3a preserved their stem cell abilities to yield differentiated progeny (maintaining multipotency), indicating that Wnt signaling has a mitogenic effect on adult retinal stem cells. It should be noted that sphere-derived cells may include retinal stem cells and committed retinal progenitor cells. Therefore, we refer to the sphere-derived cells as retinal stem/progenitor cells hereafter in this report. Wnt3a induced nuclear accumulation of β-catenin in retinal stem/progenitor cells. More strikingly, the GSK3 inhibitor SB216763, which can activate the canonical Wnt pathway, mimicked Wnt3a activity in terms of the enhancement of retinal stem/progenitor cell proliferation. These findings indicate that the canonical Wnt pathway contributes to the proliferative effect of Wnt3a on retinal stem/progenitor cells. Thus, our study provides evidence that activation of canonical Wnt signaling is useful for expanding retinal stem/progenitor cell pools in vitro. SB216763 is a less-expensive material than recombinant Wnt3a protein and could therefore reduce the cost of tissue engineering. Although the effect of another collateral pathway cannot be excluded, there is little evidence that noncanonical Wnt pathways positively regulate the cell cycle [11]. Although expression of Wnt3a was not detected in murine or avian eye [29, 30], we used commercially available recombinant Wnt3a to activate canonical Wnt pathway in this study. Recombinant Wnt3a was proved to induce self-renewal of hematopoietic stem cells by activation of canonical Wnt pathway [15], and activation of this pathway promotes proliferation of embryonic chick immature retinal cells [18].

Our study further suggests that the combination of FGF2 and Wnt3a has a strong additive effect on proliferation of adult retinal

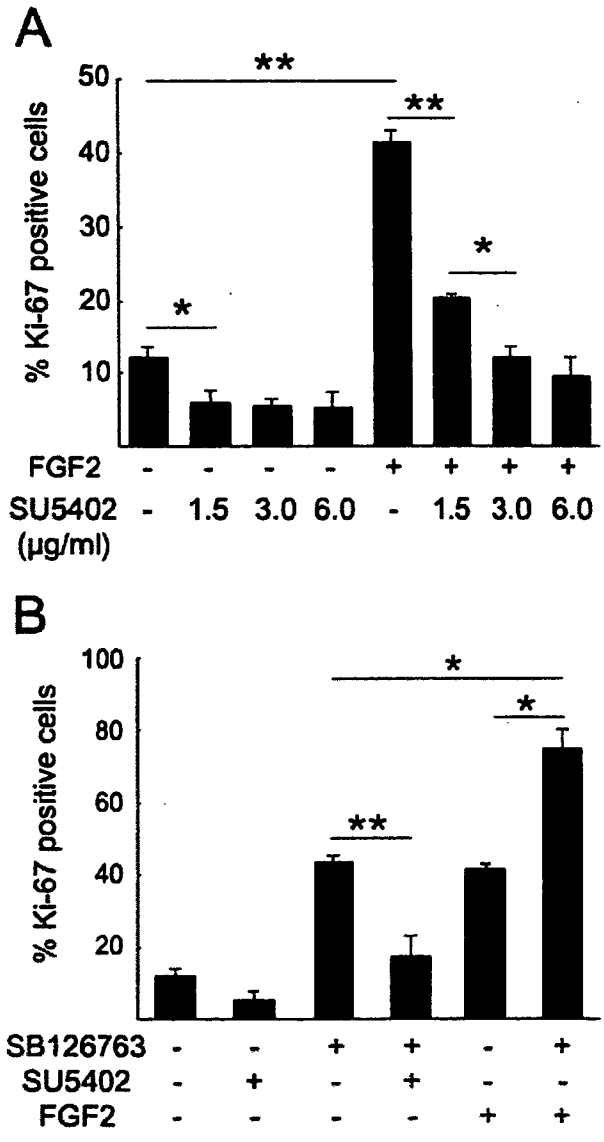

Figure 7. Effects of fibroblast growth factor 2 (FGF2) and its inhibitor on cell proliferation. The percentage of cells expressing Ki-67 was determined as described in the legend for Figure 2. Triturated sphere cells were cultured with FGF2, SU5402 (a FGF receptor inhibitor), SB216763, or their combination for 48 hours. **(A):** In the presence of exogenous FGF2, SU5402 decreases the Ki-67–positive cells in a dose-dependent manner. SU5402 decreases the Ki-67–positive cells, even in the absence of exogenous FGF2, suggesting the existence of endogenous FGF in the sphere-derived cell culture. **(B):** The effect of SB216763 on the cell proliferation is attenuated by SU5402 and enhanced by FGF2. The results are the means ± standard deviations of three replicates. $*p < .05$, $**p < .01$.

stem/progenitor cells. In the absence of endogenous FGF signaling, 7% of the total cells were Ki-67–positive. In the presence of the GSK3 inhibitor but without FGF signaling (after addition of the FGF receptor inhibitor), 18% of the total cells were Ki-67–positive (Fig. 7B). If the FGF-responsive and Wnt-responsive cells represent two different populations, 25% (7% + 18%) of the total cells should have been Ki-67–positive after the addition of the GSK3 inhibitor by itself. However, 44% of the cells were Ki67-positive, suggesting synergistic interaction between the FGF and Wnt signaling pathways. In other words, some of the retinal stem/progenitor cells showed cell cycle progression by activation of the canonical Wnt pathway that was dependent on endogenous FGF signaling. Concurrently with our present results, which we presented in the recent annual meeting of the Association for Research in Vision and Ophthalmology (Inoue T et al. , IOVS 2004;45: ARVO E-Abstract 5386), Das et al. independently showed that Wnt3a increased the number of primary spheres derived from an adult ciliary margin in the presence of FGF2 (Das AV et al. , IOVS 2004;45:ARVO E-Abstract 5396), supporting our data. AQ: 4 AQ: 5

As demonstrated in this study, the adult murine ciliary margin contains Wnt signal-responsive stem cells, although they are mitotically quiescent in vivo [31–34]. In addition, Wnt2b was reported to be expressed in the adult murine neural retina [29] and had the potential to induce proliferation of developing chick retinal precursors in vitro and in vivo via the canonical pathway [18]. The mechanism responsible for this difference between the in vivo and in vitro conditions remains unknown. N- and P-cadherin are expressed in the adult ciliary epithelium [35] and may contribute to attenuate cell proliferation by interference of the relocation of β-catenin into the nucleus (reviewed by Nelson et al. [36]). Secreted Wnt inhibitors, such as Sfrp family members expressed in the adult murine retina [29], also cannot be excluded because the roles of these molecules in the retina have not been well clarified. Another possibility is signal crosstalk with some other pathways, such as FGF signaling. The decreased FGF2 expression in the growing retina [37] could diminish the FGF-dependent proliferative effect of Wnt signaling. However, FGF2 may not actually be the partner of Wnt signaling in vivo because injured retinas were reported to express FGF2 but retinal regeneration by proliferation of retinal stem cells was not observed [38–41].

How can Wnt signaling be applied to stem cell therapy? It was recently reported that sphere cells generated from the ciliary margin could be incorporated into damaged or developing retinas, where they expressed retinal cell–specific markers, such as rhodopsin, syntaxin, and protein kinase C [42, 43]. Wnt signaling must be valuable for increasing the number of sphere colonies by continuous subcloning. Recently, Moshiri and Reh [44] reported that postnatal murine retinal margin cells showed a limited potential to regenerate retinal neurons using *patched* $(ptc)^{+/-}$ mice, in which Sonic hedgehog signaling is partially activated. In $ptc^{+/-}$ mice bred onto a retinal degeneration background, newly generated neurons and photoreceptors were observed at the retinal margin in vivo, similar to that in lower vertebrates. This observation suggests

the possibility that targeted manipulation of stem cells in the ciliary margin may lead to regeneration of damaged retinal neurons in higher vertebrates. If this is the case, the present results indicate that some molecules involved in the canonical Wnt pathway may be therapeutic targets. The effect of Wnt3a on the differentiation of the retinal stem cells derived from adult ciliary margin is not yet well clarified, and little is known about the crosstalk of Wnt signaling with the other mitotic factors for ciliary margin cells, such as insulin-like growth factor [45]. Further studies are required to fully characterize the proliferation and differentiation of retinal stem cells.

CONCLUSION

Wnt3a increased the self-renewal of retinal stem cells from the adult ciliary margin via the canonical pathway. A GSK3 inhibitor could mimic the proliferative effect of Wnt3a, which was partly dependent on FGF signaling. FGF and Wnt signaling showed a synergistic effect on retinal stem/progenitor cell proliferation, stimulating more than 75% of the total cells to become Ki-67–positive proliferating cells. These results may provide a novel therapeutic strategy for in vitro pooling or in vivo activation of retinal stem cells derived from the adult ciliary margin.

ACKNOWLEDGMENTS

The authors are very grateful to M. Ohta-Teramoto for secretarial assistance and to Y. Saiki for technical help. This work was supported by a Grant-in-Aid for 21st Century COE Research "Cell Fate Regulation Research and Education Unit" and Grant-in-Aid for Scientific Research (B) from the Ministry of Education, Culture, Sports, Science and Technology.

REFERENCES

1 Perron M, Kanekar S, Vetter ML et al. The genetic sequence of retinal development in the ciliary margin of the Xenopus eye. Dev Biol 1998; 199:185–200.

2 Wetts R, Serbedzija GN, Fraser SE. Cell lineage analysis reveals multipotent precursors in the ciliary margin of the frog retina. Dev Biol 1989;136:254–263.

3 Beach DH, Jacobson M. Patterns of cell proliferation in the retina of the clawed frog during development. J Comp Neurol 1979;183:603–613.

4 Meyer RL. Evidence from thymidine labeling for continuing growth of retina and tectum in juvenile goldfish. Exp Neurol 1978;59:99–111.

5 Johns PR. Growth of the adult goldfish eye, III: source of the new retinal cells. J Comp Neurol 1977;76:343–357.

6 Straznicky K, Gaze RM. The growth of the retina in Xenopus laevis: an autoradiographic study. J Embryol Exp Morphol 1971;26:67–79.

7 Hollyfield JG. Differential addition of cells to the retina in Rana pipiens tadpoles. Dev Biol 1968;18:163–179.

8 Ahmad I, Tang L, Pham H. Identification of neural progenitors in the adult mammalian eye. Biochem Biophys Res Commun 2000;270:517–521.

9 Tropepe V, Coles BL, Chiasson BJ et al. Retinal stem cells in the adult mammalian eye. Science 2000;287:2032–2036.

10 Engelhardt M, Wachs FP, Couillard-Despres S et al. The neurogenic competence of progenitors from the postnatal rat retina in vitro. Exp Eye Res 2004;78:1025–1036.

11 Pandur P, Maurus D, Kuhl M. Increasingly complex: new players enter the Wnt signaling network. Bioessays 2002;24:881–884.

12 Willert K, Nusse R. Beta-catenin: a key mediator of Wnt signaling. Curr Opin Genet Dev 1998;8:95–102.

13 van de Wetering M, Sancho E, Verweij C et al. The beta-catenin/TCF-4 complex imposes a crypt progenitor phenotype on colorectal cancer cells. Cell 2002;111:241–250.

14 Reya T, Duncan AW, Ailles L et al. A role for Wnt signalling in self-renewal of haematopoietic stem cells. Nature 2003;423:409–414.

15 Willert K, Brown JD, Danenberg E et al. Wnt proteins are lipid-modified and can act as stem cell growth factors. Nature 2003;423:448–452.

16 Liu BY, McDermott SP, Khwaja SS et al. The transforming activity of Wnt effectors correlates with their ability to induce the accumulation of mammary progenitor cells. Proc Natl Acad Sci U S A 2004;101:4158–4163.

17 Sato N, Meijer L, Skaltsounis L et al. Maintenance of pluripotency in human and mouse embryonic stem cells through activation of Wnt signaling by a pharmacological GSK-3-specific inhibitor. Nat Med 2004; 10:55–63.

18 Kubo F, Takeichi M, Nakagawa S. Wnt2b controls retinal cell differentiation at the ciliary marginal zone. Development 2003;130:587–598.

19 Hsieh M, Johnson MA, Greenberg NM et al. Regulated expression of Wnts and Frizzleds at specific stages of follicular development in the rodent ovary. Endocrinology 2002;143:898–908.

20 Heller RS, Dichmann DS, Jensen J et al. Expression patterns of Wnts, Frizzleds, sFRPs, and misexpression in transgenic mice suggesting a role for Wnts in pancreas and foregut pattern formation. Dev Dyn 2002;225: 260–270.

21 Tulac S, Nayak NR, Kao LC et al. Identification, characterization, and regulation of the canonical Wnt signaling pathway in human endometrium. J Clin Endocrinol Metab 2003;88:3860–3866.

22 Hoang BH, Kubo T, Healey JH et al. Expression of LDL receptor-related protein 5 (LRP5) as a novel marker for disease progression in high-grade osteosarcoma. Int J Cancer 2004;109:106–111.

23 Kee N, Sivalingam S, Boonstra R et al. The utility of Ki-67 and BrdU as proliferative markers of adult neurogenesis. J Neurosci Methods 2002; 115:97–105.

24 Hsieh JC, Rattner A, Smallwood PM et al. Biochemical characterization of Wnt-frizzled interactions using a soluble, biologically active vertebrate Wnt protein. Proc Natl Acad Sci U S A 1999;963546–3551.

25 Dann CE, Hsieh JC, Rattner A et al. Insights into Wnt binding and signalling from the structures of two Frizzled cysteine-rich domains. Nature 2001;412:86–90.

26 Cross DA, Culbert AA, Chalmers KA et al. Selective small-molecule inhibitors of glycogen synthase kinase-3 activity protect primary neurones from death. J Neurochem 2001;77:94–102.

27 Doble BW, Woodgett JR. GSK-3: tricks of the trade for a multi-tasking kinase. J Cell Sci 2003;116:1175–1186.

28 Mohammadi M, McMahon G, Sun L et al. Structures of the tyrosine kinase domain of fibroblast growth factor receptor in complex with inhibitors. Science 1997;276:955–960.

29 Liu H, Mohamed O, Dufort D et al. Characterization of Wnt signaling components and activation of the Wnt canonical pathway in the murine retina. Dev Dyn 2003;227:323–334.

30 Jin EJ, Burrus LW, Erickson CA. The expression patterns of Wnts and their antagonists during avian eye development. Mech Dev 2002;116: 173–176.

31 Cepko CL, Austin CP, Yang X et al. Cell fate determination in the vertebrate retina. Proc Natl Acad Sci U S A 1996;93:589–595.

32 Pittack C, Grunwald GB, Reh TA. Fibroblast growth factors are necessary for neural retina but not pigmented epithelium differentiation in chick embryos. Development 1997;124:805–816.

33 Feijen A, Goumans MJ, van den Eijnden-van Raaij AJ. Expression of activin subunits, activin receptors and follistatin in postimplantation mouse embryos suggests specific developmental functions for different activins. Development 1994;120:3621–3637.

34 Bodenstein L, Sidman RL. Growth and development of the mouse retinal pigment epithelium, I: cell and tissue morphometrics and topography of mitotic activity. Dev Biol 1987;121:192–204.

35 Xu L, Overbeek PA, Reneker LW. Systematic analysis of E-, N- and P-cadherin expression in mouse eye development. Exp Eye Res 2002;74: 753–760.

36 Nelson WJ, Nusse R. Convergence of Wnt, beta-catenin, and cadherin pathways. Science 2004;303:1483–1487.

37 Gao H, Hollyfield JG. Basic fibroblast growth factor in retinal development: differential levels of FGF2 expression and content in normal and retinal degeneration (rd) mutant mice. Dev Biol 1995;169:168–184.

38 Casson RJ, Chidlow G, Wood JP et al. The effect of retinal ganglion cell injury on light-induced photoreceptor degeneration. Invest Ophthalmol Vis Sci 2004;45:685–693.

39 Miyashiro M, Ogata N, Takahashi K et al. Expression of basic fibroblast growth factor and its receptor mRNA in retinal tissue following ischemic injury in the rat. Graefes Arch Clin Exp Ophthalmol 1998;236:295–300.

40 Cao W, Wen R, Li F et al. Mechanical injury increases bFGF and CNTF mRNA expression in the mouse retina. Exp Eye Res 1997;65:241–248.

41 Wen R, Song Y, Cheng T et al. Injury-induced upregulation of bFGF and CNTF mRNAS in the rat retina. J Neurosci 1995;15:7377–7385.

42 Chacko DM, Das AV, Zhao X et al. Transplantation of ocular stem cells: the role of injury in incorporation and differentiation of grafted cells in the retina. Vision Res 2003;43:937–946.

43 Coles BL, Angenieux B, Inoue T et al. Facile isolation and the characterization of human retinal stem cells. Proc Natl Acad Sci U S A 2004;101:15772–15777.

44 Moshiri A, Reh TA. Persistent progenitors at the retinal margin of $ptc^{+/-}$ mice. J Neurosci 2004;24:229–237.

45 Fischer AJ, Reh TA. Identification of a proliferating marginal zone of retinal progenitors in postnatal chickens. Dev Biol 2000;220:197–210.

Graefe's Arch Clin Exp Ophthalmol
(2006) 244: 1056–1059
DOI 10.1007/s00417-005-0238-6

SHORT COMMUNICATION

Yuki Mawatari
Akira Hirata
Mikiko Fukushima
Hidenobu Tanihara

Choroidal dye filling velocity in patients with Vogt–Koyanagi–Harada disease

Received: 14 January 2005
Accepted: 11 April 2005
Published online: 13 January 2006

Y. Mawatari · A. Hirata (✉) ·
M. Fukushima · H. Tanihara
Department of Ophthalmology and
Visual Science, Kumamoto University
Graduate School of Medical Sciences,
1–1–1 Honjo,
Kumamoto, 860-8556, Japan
e-mail: ahirata@apost.plala.or.jp
Tel.: +81-96-373-5247
Fax: +81-96-373-5249

Abstract *Purpose:* To evaluate quantitative choroidal dye filling velocity in patients with Vogt-Koyanagi-Harada disease (VKH) before and after corticosteroid treatment using indocyanine green (ICG) angiography. *Methods:* ICG angiography was performed in seven VKH patients before and after systemic corticosteroid treatment. Choroidal dye curves were obtained by image analysis software and analyzed using an exponential model. The model's time constant (τ) was used to evaluate choroidal dye filling velocity. *Results:* Compared with controls, acute phase choroidal τ values in VKH patients were significantly longer, suggesting choroidal circulation disturbance. During the recovery phase, choroidal τ values were significantly shortened, suggesting choroidal circulatory disturbance improvement. *Conclusion:* Choroidal dye filling velocity may be useful for VKH diagnosis and verification of corticosteroid treatment effectiveness.

Introduction

Vogt-Koyanagi-Harada disease (VKH) is characterized by bilateral panuveitis and systemic autoimmune disease with skin manifestations such as vitiligo and alopecia, hearing disturbances such as dysacousis and tinnitus, and meningeal signs [6]. Several studies have described characteristic ophthalmologic and angiographic findings of VKH [1, 5, 7–9, 12]. Fluorescein angiography in the acute phase of VKH has documented an area of hypofluorescence, with an early phase multiple pinpoint area of leakage and a late phase large confluent area of leakage. With indocyanine green (ICG) angiography, decreased background fluorescence and delayed filling is observed in the early phases of acute phase VKH, suggesting choroidal circulation disturbance. Corticosteroid treatment reverses these changes.

With the introduction of scanning laser ophthalmoscopes and image analyses, dye filling curves are more readily available. Using these curves, retinal and choroidal hemodynamics data have been obtained [2, 3, 11].

Choroidal circulation disturbances occur in the acute phase of VKH [1, 5, 7, 8, 12]. However, quantitative assessment of choroidal circulation has not been clarified. Therefore, we measured choroidal dye filling velocity before and after corticosteroid treatment, and investigated clinical significance.

Materials and methods

Patients

Seven patients (three males, four females) referred to and diagnosed with VKH at Kumamoto University Hospital between March 2002 and April 2003 were studied. Diagnosis was based on clinical history and ophthalmologic and related examinations, including fluorescein and ICG angiography. Patients with other systemic and ocular diseases were excluded. The mean age was 40.7±12.7 (SD) years (range 21–54 years). The mean follow-up period was 14.4±5.0 (SD) months (range, 7–20 months). Usual VKH treatments were administered with all subjects receiving intravenous betametasone (20 mg/day to 10 mg/day over 10 days) followed by oral prednisolone with cautious tapering (60 mg/day to 5 mg/day over 3 months). Prior to treatments, informed

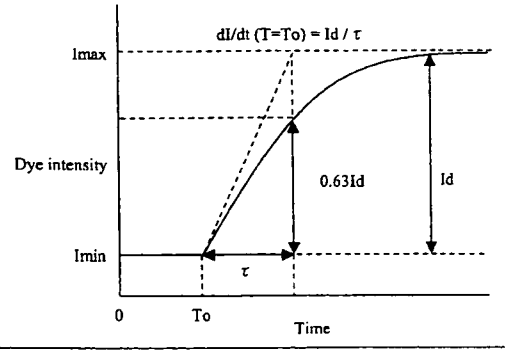

$$I(t) = Imin \quad ; 0 < T < To$$
$$= Id\{1 - EXP^{-(T-To/\tau)}\} \quad ; T \geq To$$

Imin = background intensity before appearance of the dye; To = time at the start point of the filling curves; Id = Imax – Imin, and reflects the blood volume; Imax = maximal intensity of the curve; EXP = exponent with e as the base ≅ 2.72; τ (tau) = the time constant of this model.

$$dI/dt = Id/\tau \; EXP^{-(T-To/\tau)}$$
dye filling velocity $= dI/dt\,(T = To)$
$= Id/\tau$

τ corresponds to the time of 0.63 Id of the dye curve ($1-e^{-1} \cong 0.63$).

Fig. 1 The graphical representation of the model curve used to analyze the individual dye filling curves (modified from previous report by Duijm et al. [2, 3]). The time course is described by four parameters: background intensity before appearance of the dye (*Imin*), maximal intensity of the curve (*Imax*), time at the onset of the filling curves (*To*), time constant of the model (τ)

consent was obtained from all patients in this study. Fluorescein and ICG angiography using a scanning laser ophthalmoscope (Rodenstock Instrument, Inc., Munich, Germany) were performed before initiation of, and 2 weeks and 3 months after the corticosteroid treatments. Additional angiography was performed 1 month after corticosteroid treatment in one patient suffering recurrence. As previous studies have demonstrated that the choroidal blood flow and ocular perfusion pressure relationship is linear in a certain range, each patient's blood pressure and intraocular pressure (IOP) were measured before angiograms [10]. Average ocular perfusion pressure was defined as:

$$\text{perfusion pressure} = \text{Pdiastolic} + 1/3(\text{Psystolic} - \text{Pdiastolic}) - \text{IOP}$$

Early phase angiograms were performed on one selected eye before and after corticosteroid treatment. For fluorescein angiography, 5 ml of a 10% sodium fluorescein solution was rapidly injected into the cubital vein. After fluorescein staining, 50 mg of dye (Diagnogreen; Daiichi Pharmaceutical, Inc., Tokyo, Japan) dissolved in 5 ml distilled water solution was injected into the cubital vein and ICG angiography performed. Data from angiography were analyzed using the image analysis software (DIPP-Motion2D, DITECT, Japan). The averaged intensity of targeted areas was obtained every 1/30 s and a choroidal dye curve was constructed using the software.

Controls consisted of 15 randomly selected healthy control subjects matched for age and gender. Each underwent ICG angiography after injection of 50 mg dye.

Measurement of choroidal dye filling velocity

Fluorescein angiography use in analysis of choroidal circulation has previously been presented [2, 3, 11]. We applied the same method and used ICG angiography to construct choroidal dye intensity curves. The curves were analyzed according to an exponential model shown in Fig. 1. If dye filling velocity decreases, the time constant (τ) increases. In a preliminary study, we found the choroidal τ value remained constant even when the type of dye injection changed (unpublished data from YM).

In this study, choroidal dye filling velocity was measured on macular areas that were three disk diameters in diameter and excluded large retinal vessels. The τ of each area measured was averaged.

Table 1 Clinical characteristics of VKH patients

Patient no.	Age (years)	Gender	Before treatment			After treatment					
						2 weeks			3 months		
			τ	VA	SRD	τ	VA	SRD	τ	VA	SRD
1	43	F	4.6	20/200	+	3.1	20/25	-	2.6	20/15	-
2	21	F	4.2	20/200	+	3.3	20/30	-	3.5	20/15	-
3	53	M	6	20/70	+	3.6	20/40	+	4.2	20/20	-
4	49	F	5.3	20/25	+	3.5	20/15	-	3.8	20/15	-
5	37	M	5.7	20/15	-	2.6	20/15	-	3.2	20/15	-
6	54	M	5.4	20/500	+	6.5	20/100	-	3.9	20/20	-
7	28	F	5.5	20/50	+	3.1	20/20	+	3.8	20/20	-

VA visual acuity; *SRD* serous retinal detachment

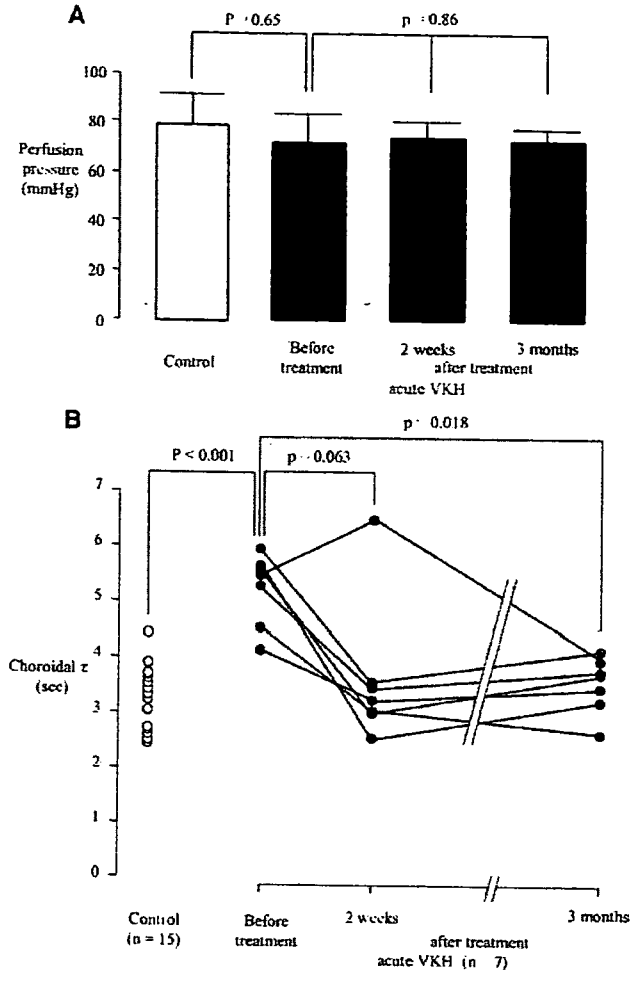

Fig. 2 Perfusion pressure and choroidal τ between control and acute VKH. **a** Compared with control, there is no difference in perfusion pressure in acute VKH. Perfusion pressure in patients with VKH was constant throughout corticosteroid therapy. **b** Compared with control, choroidal τ values in patients with acute VKH were significantly longer. Only in one patient (no. 6) was the choroidal τ value still longer at 2 weeks after corticosteroid treatment. Choroidal τ was significantly shortened in all patients at 3 months after corticosteroid treatment

Statistical analysis

Data were presented as the mean (minimal–maximal value). To compare the differences between controls and the seven acute phase VKH patients for the ocular perfusion pressure and the τ, we used an unpaired *t*-test and a Mann–Whitney *U*-test, respectively. Differences in ocular perfusion pressure before and 2 weeks and 3 months after corticosteroid treatment in the seven VKH patients were compared using repeated ANOVA and Wilcoxon signed rank sum tests. The differences in τ before and 2 weeks and 3 months after corticosteroid treatment in the seven VKH patients were compared using the Friedman test. *P*-values less than 0.05 were considered statistically significant.

Table 2 Clinical characteristics of control and VKH in acute phase

	Age (years)	Gender male : female	Perfusion pressure	τ
Control (n=15)	43.7±12.4 (28-59)	9:6	76.7±10.1 (55.0-92.3)	3.2±0.6 (2.4-4.4)
VKH in acute phase (n=7)	40.7±12.7 (21-54)	4:3	72.3±5.4 (68.0-80.0)	5.2±0.6 (4.2-6.0)

Results

In controls (n=15) matched for age and gender, average choroidal τ was 3.2 (2.4–4.4) s (Table 2). In the seven VKH acute phase patients, average choroidal τ was 5.2 (4.2–6.0) s, which was significantly longer compared to controls (Table 1, Fig. 2). There were no differences in ocular perfusion pressure between controls and the seven acute phase VKH patients (P=0.65, Table 2, Fig. 2a).

Except for subject 6, choroidal τ was shortened in all patients 2 weeks after corticosteroid treatment (Table 1, Fig. 2b). Ophthalmologic findings for this patient indicated vascular leakage during fluorescein angiography. At 2 weeks after corticosteroid treatment, an improved choroidal background was seen with ICG angiography. However, during the tapering of the corticosteroid, the patient suffered recurrence of serous retinal detachment. With increased corticosteroid administration, choroidal dye filling velocity shortened and the serous retinal detachment disappeared. In patients 3 and 7, choroidal τ values shortened without disappearance of serous retinal detachment 2 weeks after treatment (Table 1). However, the serous retinal detachments disappeared during the following week.

In the VKH recovery phase (3 months after corticosteroid treatment), choroidal τ values were significantly shortened without any noted changes in ocular perfusion pressure (P=0.018, Table 1, Fig. 2).

Discussion

In this study, we quantitatively measured choroidal circulation using ICG angiography and image analysis software. Previous studies have used fluorescein angiography to analyze choroidal circulation [2, 3, 11]. We applied this method using ICG angiography, as it reflects choroidal circulation better than fluorescein. Furthermore, we used a new type of image analysis software (DIPP-Motion 2D), which allows the dye intensity curve to easily be obtained (approximately 5–10 min per angiogram to obtain the data/curve).

Angiographic findings are useful for VKH diagnosis and evaluation of therapeutic effects [1, 5, 7–9, 12]. ICG angiography in acute phase VKH revealed a dark background, which was indistinct, and had fewer choroidal vessels and filling delays during the early phase.

We also examined the quantitative assessment of the choroidal circulation in VKH. Compared to controls, acute phase VKH patient choroidal τ values were significantly longer in the absence of ocular perfusion pressure changes, suggesting a vascular resistance increase and a disturbance of choroidal circulation during this phase. Histopathological studies of VKH in the acute phase have demonstrated that the choroid is markedly thickened and infiltrated by lymphocytes, epithelioid and giant cells [4]. Therefore, choroidal blood flow might decrease significantly, corresponding to edema or compression of the vessels by cell infiltration in the VKH acute phase. In the VKH recovery phase, choroidal τ was significantly shortened and returned to normal without changes in ocular perfusion pressure, indicating a choroidal vascular resistance decrease and improved circulation that is most likely due to the decreased inflammation.

In two patients, the choroidal τ values shortened without disappearance of serous retinal detachment. This suggests that choroidal filling velocity is not related to the presence of serous retinal detachment. In one patient, although choroidal background in the ICG seemed improved during the 2 weeks after corticosteroid treatment, the choroidal τ value was still high. With corticosteroid tapering, recurrence of serous retinal detachment was observed. Thus choroidal background improvement in ICG angiography may solely be due to disappearance of serous retinal detachment alone. However as seen in this case, the choroidal inflammation still remained and recurrence followed. This discrepancy between improvement of choroidal background and a long choroidal τ indicates that choroidal τ, which may reflect quantitative assessment of choroidal circulation, is important as an indicator of VKH treatment efficacy and as a prognostic factor for recurrence of serous retinal detachment.

Acknowledgements The authors would like to thank Drs. T. Kawaji and K. Yamada for their help.

References

1. Bouchenaki N, Herbort CP (2001) The contribution of indocyanine green angiography to the appraisal and management of Vogt-Koyanagi-Harada disease. Ophthalmology 108:54–64
2. Duijm HF, Rulo AH, Astin M, Maepea O, van den Berg TJ, Greve EL (1996) Study of choroidal blood flow by comparison of SLO fluorescein angiography and microspheres. Exp Eye Res 63:693–704
3. Duijm HF, van den Berg TJ, Greve EL (1997) A comparison of retinal and choroidal hemodynamics in patients with primary open-angle glaucoma and normal-pressure glaucoma. Am J Ophthalmol 123:644–656
4. Inomata H, Sakamoto T (1990) Immunohistochemical studies of Vogt-Koyanagi-Harada disease with sunset sky fundus. Curr Eye Res 9 Suppl:35–40
5. Kohno T, Miki T, Shiraki K, Kano K, Matsushita M, Hayashi K, De Laey JJ (1999) Subtraction ICG angiography in Harada's disease. Br J Ophthalmol 83:822–833
6. Moorthy RS, Inomata H, Rao NA (1995) Vogt-Koyanagi-Harada syndrome. Surv Ophthalmol 39:265–292
7. Okada AA, Mizusawa T, Sakai J, Usui M (1998) Videofunduscopy and videoangiography using the scanning laser ophthalmoscope in Vogt-Koyanagi-Harada syndrome. Br J Ophthalmol 82:1175–1181
8. Oshima Y, Harino S, Hara Y, Tano Y (1996) Indocyanine green angiographic findings in Vogt-Koyanagi-Harada disease. Am J Ophthalmol 122:58–66
9. Pece A, Bolognesi G, Introini U, Brancato R (1997) Indocyanine green angiography in Vogt-Koyanagi-Harada-type disease. Arch Ophthalmol 115:804–806
10. Riva CE, Titze P, Hero M, Petrig BL (1997) Effect of acute decreases of perfusion pressure on choroidal blood flow in humans. Invest Ophthalmol Vis Sci 38:1752–1760
11. van Stokkum IH, Lambrou GN, van den Berg TJ (1995) Hemodynamic parameter estimation from ocular fluorescein angiograms. Graefe's Arch Clin Exp Ophthalmol 233:123–130
12. Yuzawa M, Kawamura A, Matsui M (1993) Indocyanine green video-angiographic findings in Harada's disease. Jpn J Ophthalmol 37:456–466

Another feature of CGD involves poor wound healing.[10] Therefore, subretinal granulation tissue mass in our case may represent an abnormal reparative response to previous chorioretinal injury. The absence of infection or granuloma, intravitreal pro-inflammatory cytokines, and improvement with immunosuppression suggests that his ocular disease is probably the result of aberrant inflammatory responses. Routine ocular biopsy is not recommended as part of standard ophthalmic evaluation.

R R Buggage
Laboratory of Immunology, National Eye Institute, National Institute of Allergy and Infectious Diseases, National Institutes of Health, Bethesda, MD, USA

R M Bauer II
Winn Army Hospital, Fort Stewart, GA, USA

S M Holland
Laboratory of Host Defenses, National Institute of Allergy and Infectious Diseases, National Institutes of Health, Bethesda, MD, USA

C I Santos
Department of Ophthalmology, University of Puerto Rico, San Juan, Puerto Rico

C-C Chan
Laboratory of Immunology, National Eye Institute, National Institute of Allergy and Infectious Diseases, National Institutes of Health, Bethesda, MD, USA

Correspondence to: Chi-Chao Chan, MD, National Eye Institute, National Institutes of Health, 10 Center Drive, Bldg 10, Room 10N103, Bethesda, MD 20892-1857, USA; chanc@nei.nih.gov

doi: 10.1136/bjo.2005.081505

Accepted for publication 1 November 2005

Financial support: Intramural program of the National Eye Institute, NIH.

References

1 **Segal BH**, Leto TL, Gallin JI, *et al.* Genetic, biochemical, and clinical features of chronic granulomatous disease. *Medicine (Baltimore)* 2000;**79**:170–200.
2 **Johnston RB Jr.** Clinical aspects of chronic granulomatous disease. *Curr Opin Hematol* 2001;**8**:17–22.
3 **El-Benna J**, Dang PM, Gougerot-Pocidalo MA, *et al.* Phagocyte NADPH oxidase: a multicomponent enzyme essential for host defenses. *Arch Immunol Ther Exp (Warsz)* 2005;**53**:199–206.
4 **Clark RA**, Malech HL, Gallin JI, *et al.* Genetic variants of chronic granulomatous disease: prevalence of deficiencies of two cytosolic components of the NADPH oxidase system. *N Engl J Med* 1989;**321**:647–52.
5 **Palestine AG**, Meyers SM, Fauci AS, *et al.* Ocular findings in patients with neutrophil dysfunction. *Am J Ophthalmol* 1983;**95**:598–604.
6 **Goldblatt D**, Butcher J, Thrasher AJ, *et al.* Chorioretinal lesions in patients and carriers of chronic granulomatous disease. *J Pediatr* 1999;**134**:780–3.
7 **Djalilian AR**, Smith JA, Walsh TJ, *et al.* Keratitis caused by Candida glabrata in a patient with chronic granulomatous disease. *Am J Ophthalmol* 2001;**132**:782–3.
8 **Valluri S**, Chu FC, Smith ME. Ocular pathologic findings of chronic granulomatous disease of childhood. *Am J Ophthalmol* 1995;**120**:120–3.
9 **Grossniklaus HE**, Frank KE, Jacobs G. Chorioretinal lesions in chronic granulomatous disease of childhood. Clinicopathologic correlations. *Retina* 1988;**8**:270–4.
10 **Eckert JW**, Abramson SL, Starke J, *et al.* The surgical implications of chronic granulomatous disease. *Am J Surg* 1995;**169**:320–3.

Ocular decompression retinopathy following trabeculectomy with mitomycin C associated with familial amyloidotic polyneuropathy

Familial amyloidotic polyneuropathy (FAP), a disorder inherited in autosomal dominant fashion, is characterised by systemic accumulation of polymerised mutated amyloidogenic TTR (ATTR) in peripheral nerves and in organs.[1] We report two patients with FAP ATTR Y114C (a point mutation, from tyrosine to cysteine, at codon 114) who developed diffuse retinal haemorrhages immediately after uncomplicated trabeculectomy with mitomycin C (MMC).

Case reports

A woman underwent vitrectomy for vitreous opacity associated with FAP ATTR Y114C in the left eye when she was 34 years old and in the right eye when she was 35 years old. Neurological examination revealed that she had polyneuropathy and autonomic dysfunction, and she underwent liver transplantation at 34 years old. Thereafter, intraocular pressure (IOP) in the left eye gradually increased and visual field loss progressed. Trabeculectomy with MMC in the left eye was performed when she was 39 years old. Preoperative IOP was 43 mm Hg despite maximal medical therapy. On the next postoperative day, IOP was 5 mm Hg, and fundus examination revealed scatter retinal haemorrhages in the periphery and posterior pole (fig 1). The haemorrhages had completely resolved and visual acuity was 20/20 in the left eye.

A woman underwent vitrectomy for vitreous opacity associated with FAP ATTR Y114C when she was 45 and trabeculectomy in the right eye at another hospital when she was 46, respectively. At 48, vitrectomy in the left eye was performed. She underwent liver transplantation at 50. Thereafter, IOP in the left eye gradually increased and non-penetrating trabeculectomy with MMC was performed when she was 51. However, IOP increased postoperatively, and trabeculectomy with MMC was added. IOP before the additional trabeculectomy was 37 mm Hg despite maximal medical therapy. On the next postoperative day, IOP was 5 mm Hg, and fundus examination revealed scatter retinal haemorrhages in the periphery and posterior pole involving the fovea. Although haemorrhages had almost resolved during the follow up period, visual acuity decreased from 20/20 to 20/50.

Comment

Retinal haemorrhages are a rare complication after filtration surgery.[2–6] Fechtner *et al* reported this condition for the first time under the descriptive term of ocular decompression retinopathy.[2] Affected patients are typically young, but not exclusively, with relatively high preoperative IOP, a very low postoperative IOP, and advanced cupping. Elevated IOP levels are generally significantly high in cases of secondary glaucoma related to FAP,[7] and diffuse retinal haemorrhages immediately after uncomplicated trabeculectomy with MMC are noted in both cases. One possible mechanism is hypothesised to be caused by a loss of autoregulation of retinal vessels, which overwhelms their capacity to respond to changes in IOP, resulting in retinal haemorrhages.[2] Our cases had an autonomic dysfunction as a systemic symptom, further increasing the susceptibility to such a phenomenon. Also, although both

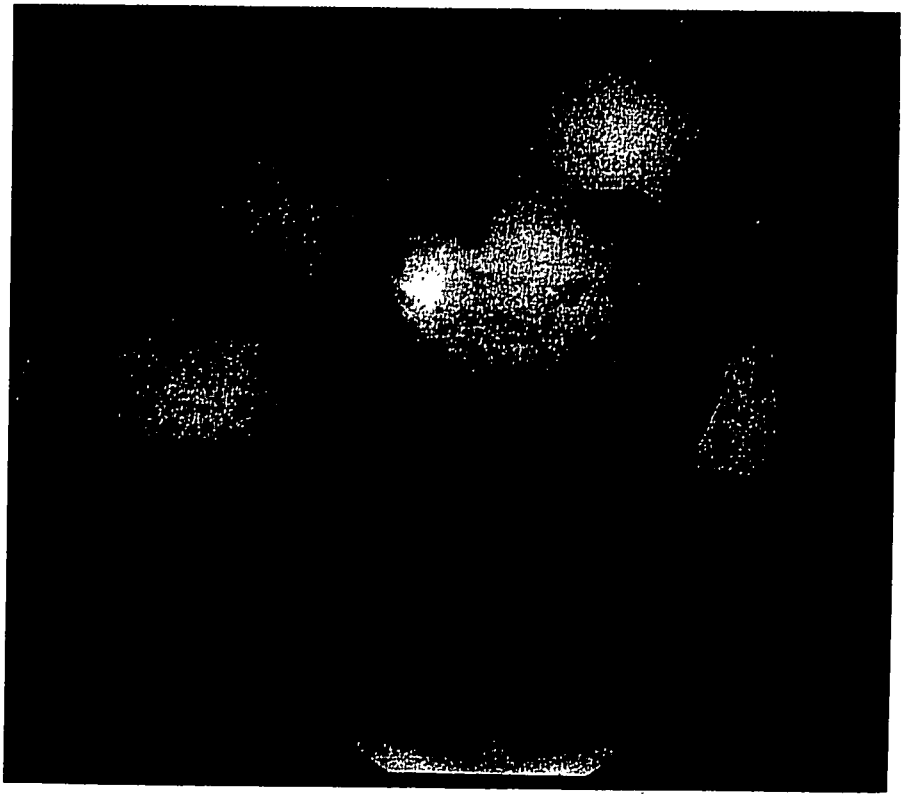

Figure 1 Scatter retinal haemorrhages in the periphery and posterior pole on the first postoperative day.

cases underwent trabeculectomy after vitrectomy, there were no complications, such as the collapse of eye, caused by a vitreous condition. Visual prognosis is usually benign after the resolution of haemorrhages; however, cases with poor visual acuity as shown in case 2 have also been described. Taken together, because clinical features in glaucoma secondary to FAP are related to the pathogenesis of this rare complication after trabeculectomy, early postoperative hypotony should be avoided to prevent it.

Acknowledgements

The authors' work was supported in part by a grant in aid for scientific research from the Ministry of Education, Science, Sports and Culture, Japan, from the Ministry of Health and Welfare, Japan.

M Wakita, T Kawaji, E Ando, T Koga, M Inatani, H Tanihara
Department of Ophthalmology and Visual Science, Graduate School of Medical Sciences, Kumamoto University, 1-1-1 Honjo, Kumamoto 860-8556, Japan

Y Ando
Department of Diagnostic Medicine, Graduate School of Medical Sciences, Kumamoto University, 1-1-1 Honjo, Kumamoto 860-8556, Japan

Correspondence to: Takahiro Kawaji, MD, Ophthalmology and Visual Science, Graduate School of Medical Sciences, Kumamoto University, 1-1-1 Honjo, Kumamoto 860-8556, Japan; kawag@white.plala.or.jp

doi: 10.1136/bjo.2005.082735

Accepted for publication 1 November 2005

References

1 **Araki S.** [Type I familial amyloidotic polyneuropathy]. *No To Hattatsu* 1984;**16**:92–100.
2 **Fechtner RD**, Minckler D, Weinreb RN, *et al.* Complications of glaucoma surgery. Ocular decompression retinopathy. *Arch Ophthalmol* 1992;**110**:965–8.
3 **Dudley DF**, Leen MM, Kinyoun JL, *et al.* Retinal hemorrhages associated with ocular decompression after glaucoma surgery. *Ophthalmic Surg Lasers* 1996;**27**:147–50.
4 **Suzuki R**, Nakayama M, Satoh N. Three types of retinal bleeding as a complication of hypotony after trabeculectomy. *Ophthalmologica* 1999;**213**:135–8.
5 **Danias J**, Rosenbaum J, Podos SM. Diffuse retinal hemorrhages (ocular decompression syndrome) after trabeculectomy with mitomycin C for neovascular glaucoma. *Acta Ophthalmol Scand* 2000;**78**:468–9.
6 **Dev S**, Herndon L, Shields MB. Retinal vein occlusion after trabeculectomy with mitomycin C. *Am J Ophthalmol* 1996;**122**:574–5.
7 **Kimura A**, Ando E, Fukushima M, *et al.* Secondary glaucoma in patients with familial amyloidotic polyneuropathy. *Arch Ophthalmol* 2003;**121**:351–6.

Dapsone induced haemolytic anaemia in patients treated for ocular cicatricial pemphigoid

Ocular cicatricial pemphigoid (OCP) is a systemic autoimmune disease of unknown aetiology. It causes a chronic, scarring conjunctivitis and frequently affects other mucous membranes. Definitive diagnosis is made by immunofluorescent staining of conjunctival tissue demonstrating IgG, IgM, and or IgA in the basement membrane.[1] Dapsone is an immunomodulating sulphonamide and has widely been used in the treatment of mild to moderate OCP.[2–4] All patients treated with dapsone show varying degrees of haemolysis.[5] Haemolytic anaemia, requiring withdrawal of therapy, has been shown to occur in approximately 10% of patients.[2 5]

The medical records of 12 patients treated with dapsone for ocular cicatricial disease were reviewed. Eleven of these patients were treated with dapsone as first line therapy and one as second line therapy; 11 patients had ocular cicatricial pemphigoid (OCP) and one had idiopathic cicatrising disease. There were an equal number of male and females in this group with a mean age of 72 years (range 55–89 years). The daily dose of dapsone was consistent at 50 mg twice daily taken orally. Mean follow up time while on dapsone therapy was 19 months with a range of 1–60 months.

Six (50%) patients had reticulocytosis including four (33%) with clinically significant haemolytic anaemia with a raised mean cell volume and a steady fall in haemoglobin from baseline. The development of the haemolytic anaemia was not dose dependent and all the patients had a diagnosis of OCP (table 1).

Our cohort of patients had a much higher rate of haemolytic anaemia than previously published reports.[2 5] Although our study sample is small, the proportion of patients with haemolytic anameia is striking. Patients who are glucose-6-phosphate hydrogenase (G6PD) deficient are known to be more at risk of developing haemolytic anaemia.[4] We do not routinely check for this rare deficiency in our department. Clinically significant dapsone induced haemolytic anaemia may occur more frequently than previously expected and clinicians should be acutely aware of any downward trend in haemoglobin from baseline. We no longer use dapsone as a first line agent in the management of OCP.

M S Wertheim, J J Males, S D Cook, D M Tole
Bristol Eye Hospital, Lower Maudlin Street, Bristol BS1 2LX, UK

Correspondence to: Michael S Wertheim, Bristol Eye Hospital, Lower Maudlin Street, Bristol BS1 2LX, UK; drwertie@hotmail.com

doi: 10.1136/bjo.2005.085837

Accepted for publication 3 December 2005

The authors have no competing interests.

References

1 **Chiou AG**, Florakis GJ, Kazim M. Management of conjunctival cicatrizing diseases and severe ocular surface dysfunction. *Surv Ophthalmol* 1998;**43**:19–46.
2 **Doan S**, Lerouic JF, Robin H, *et al.* Treatment of ocular cicatricial pemphigoid with sulfasalazine. *Ophthalmology* 2001;**108**:1565–8.
3 **Rogers RS 3rd**, Seehafer JR, Perry HO. reatment of cicatricial (benign mucous membrane) pemphigoid with dapsone. *J Am Acad Dermatol* 1982;**6**:215–23.
4 **Tauber J**, Sainz de la Maza M, Foster CS. Systemic chemotherapy for ocular cicatricial pemphigoid. *Cornea* 1991;**10**:185–95.
5 **Foster CS.** Cicatricial pemphigoid. *Trans Am Ophthalmol Soc* 1986;**84**:527–663.

Bilateral juxtapapillary choroidal neovascularisation associated with interferon alfa treatment of a metastatic cutaneous melanoma

Interferon alfa (IFNα) is commonly used in the treatment of many neoplastic diseases owing to its antiproliferative and immunomodulatory effects. IFNα is used in adjuvant therapy of melanoma stage IIa/b or higher.[1] A wide variety of ocular adverse events related to IFN therapy have been reported during the past decades.[2 3] A case of bilateral juxtapapillary choroidal neovascularisation is described here.

Case report

A 48 year old woman reported acute vision loss in her left eye (LE) 1 week after starting treatment with IFNα for a cutaneous metastasic melanoma. She had been receiving IFNα, 5 million international units (MIU), subcutaneously three times a week. On examination, visual acuity (VA) was right eye (RE) 20/50 and LE 20/60. Funduscopy showed bilateral optic disc oedema and subretinal haemorrhages in inferior temporal and nasal arcades. To rule out any cause of papilloedema a brain computed tomography was performed, which was normal. One month later, IFNα doses were increased to 8 MIU; VA decreased to RE 20/100 and LE counting fingers at 9 feet. Funduscopy showed bilateral optic disc oedema, bilateral juxtapapillary serous retinal detachment, and subretinal haemorrhages (fig 1A, B).

Table 1 Patients with haematological complications from dapsone

Patient	Age (years)	Sex	Diagnosis	Dapsone dose	Complication
1	77	M	OCP	50 mg twice daily	Reticulocytosis (with normal Hb)
2	78	M	OCP	50 mg twice daily	Haemolytic anaemia*
3	67	M	OCP	50 mg twice daily	Reticulocytosis (with normal Hb)
4	60	F	OCP	50 mg twice daily	Haemolytic anaemia*
5	89	F	OCP	50 mg twice daily	Haemolytic anaemia*
6	85	F	OCP	50 mg twice daily	Haemolytic anaemia*

OCP, ocular cicatricial pemphigoid, Hb, haemoglobin, *dapsone withdrawn.

Posterior Vitreous Detachment Induced by Nattokinase (Subtilisin NAT): A Novel Enzyme for Pharmacologic Vitreolysis

Akiomi Takano,[1] *Akira Hirata,*[1] *Kazuya Ogasawara,*[2] *Nina Sagara,*[1] *Yasuya Inomata,*[1] *Takahiro Kawaji,*[1] *and Hidenobu Tanihara*[1]

Purpose. To investigate the effects of intravitreal injection of nattokinase (subtilisin NAT), a serine protease that is produced by *Bacillus subtilis* (natto), for induction of posterior vitreous detachment (PVD).

Methods. Different doses of nattokinase (1, 0.1, or 0.01 fibrin-degradation units [FU]) or physiologic saline as a control were injected into the vitreous cavity of rabbit eyes. Scanning electron microscopy was used to observe the retinal surfaces of four rabbit eyes per concentration. Histologic alterations were assessed by light microscopy, using four eyes from each group. Electroretinography (ERG) was performed to observe retinal function, ranging from 1 hour to 1 week after the nattokinase (1 or 0.1 FU) or saline solution administration, using four eyes from each group at each time point. Also, findings in all rabbits were monitored by slit lamp examination and by indirect ophthalmoscopy with a 20-D lens.

Results. Scanning electron microscopy showed smooth retinal surfaces, indicating the occurrence of PVD at 30 minutes after intervention in all the experimental eyes injected with 0.1 or 1.0 FU nattokinase, but none of the control eyes. Light microscopy and ERG analysis showed no critical change even after the use of 0.1 FU nattokinase, an amount sufficient to induce PVD. However, toxicity in the forms of preretinal hemorrhage and ERG changes was noted with the higher dose (1 FU) of nattokinase.

Conclusions. The results suggested that nattokinase is a useful enzyme for pharmacologic vitreolysis because of its efficacy in inducing PVD. (*Invest Ophthalmol Vis Sci.* 2006;47: 2075–2079) DOI:10.1167/iovs.05-0130

From the [1]Department of Ophthalmology and Visual Science, Kumamoto University Graduate School of Medical Sciences, Kumamoto, Japan; and the [2]Japan Bio Science Laboratory Co:, Ltd., Oita, Japan.

Supported in part by Grants-in-Aid for Scientific Research from the Ministry of Education, Science, Sports and Culture, Japan, and from the Ministry of Health and Welfare, Japan.

Submitted for publication February 1, 2005; revised April 27, September 15, and December 28, 2005; accepted March 13, 2006.

Disclosure: **A. Takano**, Japan Bio Science Laboratory Co., Ltd. (F,P); **A. Hirata**, Japan Bio Science Laboratory Co., Ltd. (F,P); **K. Ogasawara**, Japan Bio Science Laboratory Co., Ltd. (E); **N. Sagara**, Japan Bio Science Laboratory Co., Ltd. (F); **Y. Inomata**, Japan Bio Science Laboratory Co., Ltd. (F); **T. Kawaji**, Japan Bio Science Laboratory Co., Ltd. (F); **H. Tanihara**, Japan Bio Science Laboratory Co., Ltd. (F,P)

The publication costs of this article were defrayed in part by page charge payment. This article must therefore be marked "*advertisement*" in accordance with 18 U.S.C. §1734 solely to indicate this fact.

Corresponding author: Hidenobu Tanihara, Department of Ophthalmology and Visual Science, Kumamoto University Graduate School of Medical Sciences, 1-1-1 Honjo, Kumamoto 860-8556, Japan; tanihara@pearl.ocn.ne.jp.

Investigative Ophthalmology & Visual Science, May 2006, Vol. 47, No. 5

The vitreous is composed of a network of two major constituents, collagen, and hyaluronan.[1] In patients with proliferative vitreoretinal disorders, the formation and recurrence of proliferative tissue at the vitreoretinal interface often cause a high incidence of vitreous hemorrhage, retinal detachment, and resultant visual loss after vitreous surgeries. The current treatment for vision-threatening proliferative vitreoretinal diseases consists of vitrectomy to remove the proliferative tissue and its scaffold of vitreous from the retinal surface surgically.

However, the surgical procedure for the creation of posterior vitreous detachment (PVD) is associated with a potential risk of the onset of retinal breaks and hemorrhage. In addition, even after vitreous surgeries, the occurrence and progression of cell proliferation on the residual vitreous gel sometimes cause serious postoperative complications, such as proliferative vitreoretinopathy (PVR). Therefore, the development of an enzymatic treatment for the complete removal of the vitreous (and associated proliferative tissue) is desirable, to reduce the incidence of complications during and after vitreous surgeries.[2–5]

The vitreous is composed mainly of collagen and hyaluronan; therefore, hyaluronidase has been recommended for intravitreal injection to facilitate vitreous liquefaction and vitreous hemorrhage absorption.[6,7] Plasmin has been also reported to be an effective adjunct for the induction of PVD.[8–14] Previous reports on the clinical use of plasmin purified from autologous blood showed the usefulness of enzyme-assisted vitrectomy for vitreoretinal diseases.[15–18]

Nattokinase (subtilisin NAT) is a serine protease composed of 275 amino acids that is produced by *Bacillus subtilis* (natto).[19] It has potent fibrinolytic activity, enhances plasminogen activators, and inactivates a plasminogen activator inhibitor.[20–22] It also has fibrinolytic activity when administered orally and is widely available in processed and health foods containing natto (fermented soybean) extracts.[21] Therefore, we hypothesized that nattokinase might be an effective pharmacologic adjunct to surgery to induce PVD in patients with vitreoretinal disorders.

In the present study, we determined the efficacy and the safety of nattokinase for pharmacologic vitreolysis.

Materials and Methods

Experimental Animals

Japanese adult albino rabbits (Kyudo, Kumamoto, Japan), 12 weeks old and weighing 2.0 kg, were used in the study. The animals were treated in accordance with the ARVO Statement for the Use of Animals in Ophthalmic and Vision Research and the guidelines of the Committee on Animal Research of Kumamoto University.

Nattokinase Preparation

Nattokinase was supplied by Japan Bio Science Laboratory Co., Ltd. (JBSL; Oita, Japan). It was purified from fermented soybean extract

(product name NSK-SD; JBSL) including rich nattokinase produced by *B. subtilis* (natto), as follows. The fermented soybean extract (NSK-SD) was dissolved in 2 mM calcium acetate, dialyzed overnight in 10 mM phosphate buffer (pH 7.0), adsorbed on a pre-equilibrated Sepharose column (CM-Sepharose Fast Flow; GE Healthcare, Piscataway, NJ), and finally washed and eluted with a linear gradient of 10 mM phosphate buffer (pH 7.0) containing 500 mM sodium chloride. To obtain the active enzyme fraction, the sample was gel-filtrated in a Sephacryl column (S-100 HR; GE Healthcare) equilibrated with 10 mM phosphate buffer (pH 7.5) containing 150 mM of sodium chloride. The active enzyme fraction was electrophoresed on a sodium dodecyl sulfate-polyacrylamide gel and confirmed as a single band.

Nattokinase Activity

Nattokinase activity was measured with a fibrin degradation assay developed by JBSL. First, 0.4 mL of 0.72% fibrinogen (fibrinogen fraction I, type I-S, product number F8630; Sigma-Aldrich, St. Louis, MO) was placed in a test tube (15-mm inner diameter × 150-mm length) with 1.4 mL of 50 mM borate buffer (pH 8.5) containing 0.9% sodium chloride and incubated in a constant-temperature water bath at 37 ± 0.3°C for 5 minutes. Then, 0.1 mL of a 20-U/mL thrombin solution (product number T6634; Sigma-Aldrich) was added. The solution was incubated at 37 ± 0.3°C for exactly 10 minutes, 0.1 mL of sample solution was added, and incubation continued at 37 ± 0.3°C. This solution was again mixed after 20 and 40 minutes. At exactly 60 minutes, 2 mL of 200 mM trichloroacetic acid was added, mixed, and the solution was incubated at 37 ± 0.3°C for 20 minutes. This solution was placed in a microcentrifuge tube and centrifuged at 15,000*g* for 5 minutes. Then, 1 mL of supernatant was collected and the absorbance at 275 nm was measured. In this assay, 1 unit (fibrin degradation unit, FU) of enzyme activity is defined as a 0.01-per-minute increase in absorbance at 275 nm of the reaction solution (excluding acid-insoluble material).

The substrate (fibrinogen) used in this assay is naturally derived, and so there can be considerable differences in quality among product lots. This makes it difficult to determine absolute values for enzyme activity. Therefore, JBSL also supplies a standard enzyme for use in the assay. The measured value divided by the labeled standard enzyme activity was used as a correction factor. All assay values were then multiplied by this correction factor. Measurement of human plasmin activity by this assay showed that 1 unit of human plasmin (Calbiochem, La Jolla, CA) had an activity equivalent to 1 FU. These activities were measured by JBSL, and the prepared nattokinase was used immediately after measurement of the activity.

Anesthesia

The rabbits were anesthetized for each procedure with pentobarbital (20 mg/kg injected intravenously) and ketamine hydrochloride (20 mg/kg injected intramuscularly).

Administration of Nattokinase

Rabbits were randomized into four groups. Group 1 received 1 FU nattokinase, group 2 received 0.1 FU, group 3 received 0.01 FU, and group 4 received physiologic saline (BSS Plus; Alcon Surgical, Tokyo, Japan) in one eye. The pupils were dilated with a mixture of 0.5% tropicamide and 0.5% phenylephrine hydrochloride. Nattokinase activity was adjusted by dilution with physiologic saline. After filter sterilization using a 0.22-μm membrane filter, 1-mL syringes of nattokinase dilutions were prepared (1 FU/0.1 mL, 0.1 FU/0.1 mL, and 0.01 FU/0.1 mL). A vitrectomy contact lens was placed on the cornea, then under an ophthalmic microscope, a 30-gauge needle attached to a syringe was inserted at a point 2 mm from the corneal limbus. Then, 0.1 mL of nattokinase solution was carefully and slowly injected into the center of the vitreous cavity. Control eyes were injected in a similar manner with 0.1 mL physiologic saline. Because of increased intraocular pressure after injection, anterior chamber paracentesis was performed immediately with a 20-gauge ophthalmic knife to normalize the pressure and prevent the solution from coming out of the eye.

Scanning Electron Microscopy

Sixteen eyes were studied with scanning electron microscopy (SEM). Nattokinase (1, 0.1, or 0.01 FU) or saline was injected into the vitreous cavity of four rabbit eyes per concentration. At 30 minutes after injection, the eyes were enucleated and fixed with a mixture of 2.5% glutaraldehyde and 2% paraformaldehyde in 100 mM phosphate buffer at 4°C. One hour later, the eyes were cut circumferentially at the limbus to make posterior cups and then placed in fixative solution (the same one as above) overnight. The posterior cup was cut across and vertically with a razor to prepare samples for SEM. The samples were placed in 2% tannic acid (Wako Pure Chemicals, Osaka, Japan) and allowed to stand overnight at 4°C. Then, the samples were washed six times with phosphate-buffered saline at 20-minute intervals, placed in 2% osmium on ice, and allowed to stand for 70 minutes. After recovery of the 2% osmium, the samples were washed three times with distilled water, dehydrated in an ethanol series (50% for 15 minutes, 70% for 15 minutes, 90% for 15 minutes, 95% for 15 minutes, and twice in 99.5% for 30 minutes), and immersed in *t*-butyl alcohol (20 minutes, three times). After freezing, the samples were freeze dried, mounted on an aluminum stage with double-sided carbon tape, coated with gold (JFC-1200; JEOL, Tokyo, Japan), and examined with a scanning electron microscope (JSM-5800 LV; JEOL).

Light Microscopy and Electroretinography

To evaluate the short-term effects of intraocular injection of nattokinase, 30 minutes after intravitreal injection of nattokinase (1, 0.1, or 0.01 FU) or saline solution as a control, four eyes from each group were used for a light microscopic study of the retina. The eyes were fixed with a mixture of 2.5% glutaraldehyde and 2% paraformaldehyde in 100 mM phosphate buffer for 24 hours and embedded in paraffin, and horizontal sections were made and stained with hematoxylin and eosin.

Also, to investigate the adverse effects of nattokinase, we obtained scotopic full-field electroretinograms (ERGs) at times ranging from 1 hour to 1 week after the nattokinase (1 or 0.1 FU) or saline administration, using four eyes from each group at each time point. The pupils were dilated and dark adapted for 30 minutes before recordings. White-light-emitting diode built-in contact lens electrodes (LW-102; Tomey, Waltham, MA) were put on the cornea, and an electrode was attached to the forehead after the hair was shaved from the area. A ground electrode was attached to the ear. Stimuli (6000 cd/m^2, 0.5 ms) were delivered, and ERGs were recorded (LE-2000; Tomey). Statistical analyses were performed on a computer (StatView, ver. 5.0; SAS Institute, Inc., Cary, NC). In addition, a light microscopic study of the retina was performed 1 week after the administration of 1 or 0.1 FU nattokinase or saline solution in four eyes from each group.

Slit Lamp Examination and Indirect Ophthalmoscopy

Findings in all rabbits were monitored by slit lamp examination and by indirect ophthalmoscopy with a 20-D lens.

Results

Scanning Electron Microscopy

Figure 1 shows an example of the retinal surface observed by SEM. In all the saline-injected eyes, SEM showed very dense vitreous fibers covering the entire area of the retinal surface (Fig. 1, top left). All eyes treated with 0.01 FU nattokinase still showed numerous vitreous fibers covering the retinal surface (Fig. 1, top right). These fibers were attached to the retina, particularly in the area of the medullary rays. In contrast, all eyes in the groups treated with 0.1 or 1 FU nattokinase exhib-

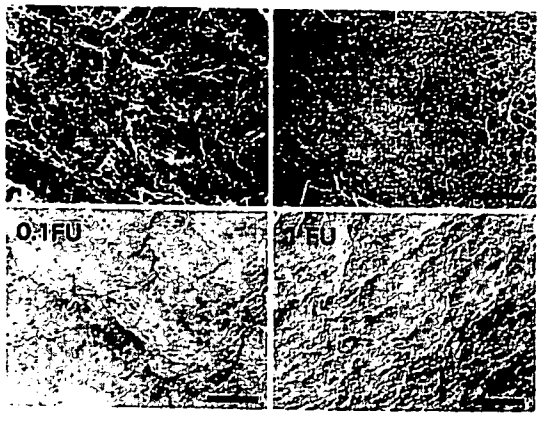

FIGURE 1. Scanning electron microscopy (SEM) image of the retinal surface 30 minutes after an intravitreal injection of physiologic saline (*top left*) or 0.01 (*top right*), 0.1 (*bottom left*), or 1 (*bottom right*) FU nattokinase. In the saline-injected eyes, SEM showed very dense vitreous fibers covering the retinal surface. In contrast, the eyes treated with 0.1 or 1 FU nattokinase exhibited smooth retinal surfaces, indicating the occurrence of posterior vitreous detachment. Bar, 50 μm.

ited smooth retinal surfaces without any remnant of vitreous fibers, except in the regions of the medullary rays (Fig. 1, bottom).

Light Microscopy and ERG

Figure 2 shows an example of the retinal section 30 minutes after the administration of nattokinase. All eyes showed intact retinal surfaces and no abnormalities compared with control eyes.

Figure 3 shows the ERG findings for tested eyes. The ERG a- and b-waves in control eyes showed no significant reductions in the mean amplitudes from the preoperative examination ($P > 0.1$). In eyes treated with 0.1 FU nattokinase, the a-wave showed no significant reductions. Temporary reduction of the b-wave was observed 1 day after the administration of 0.1 FU nattokinase ($P = 0.021$); however, amplitude recovered 1 week after the intervention ($P = 0.170$). In eyes injected with 1 FU nattokinase, the b-wave amplitude 1 day and 1 week after injection showed significant reductions ($P = 0.012$ and 0.045, respectively). The a-wave 1 week after injection also showed significant reduction ($P = 0.006$). The histology of the retina 1 week after administration of saline solution or 0.1 FU nattokinase showed no adverse change. One week after 1 FU nattokinase, however, slight thinning of the inner plexiform layer was observed (Fig. 4).

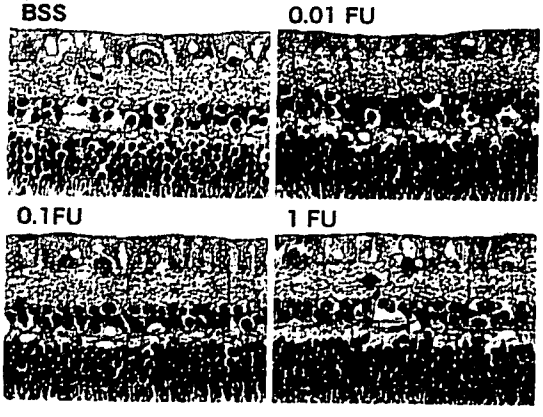

FIGURE 2. Light micrograph of rabbit retinas 30 minutes after an intravitreal injection of saline solution (*top left*) or 0.01 (*top right*), 0.1 (*bottom left*), or 1 (*bottom right*) FU nattokinase. There were no abnormalities compared with the control eyes. Magnification, ×400.

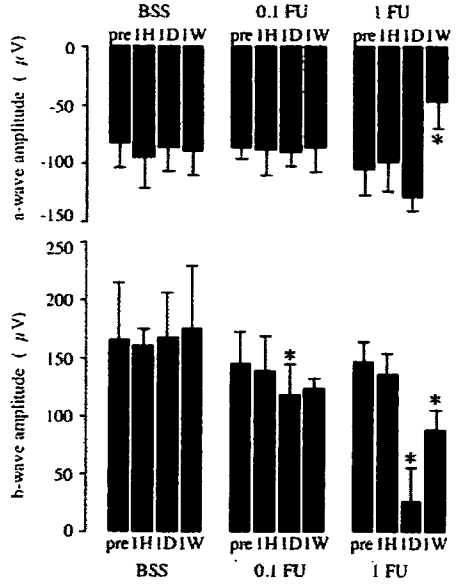

FIGURE 3. The mean (±SD) of ERG a- and b-waves before and after nattokinase injection (*$P < 0.05$). Data are shown for injection of physiologic saline or 0.1 or 1 FU nattokinase. pre, before injection; 1 H, 1 hour; 1 D, 1 day; and 1 W, 1 week after injection.

Slit Lamp Examination and Indirect Ophthalmoscopy

Slit lamp examination and indirect ophthalmoscopy during follow-up showed no evidence of hemorrhage, retinal detach-

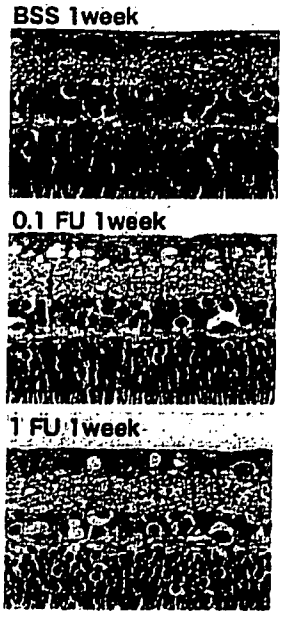

FIGURE 4. Light micrograph of rabbit retinas 1 week after an intravitreal injection of saline solution (*top*) or 0.1 (*middle*) or 1 FU nattokinase (*bottom*). Histology 1 week after the administration of saline or 0.1 FU nattokinase showed no adverse change. One week after injection of 1 FU nattokinase, however, slight thinning of the inner plexiform layer was observed. Magnification, ×400.

ment, or any other complications after the use of 0.01 FU nattokinase in all the tested eyes. Also, all eyes injected with 0.1 FU nattokinase, which was sufficient to induce PVD, showed no abnormalities compared with control eyes. However, 1 day after injection of 1 FU nattokinase, we observed mild preretinal hemorrhages near the optic disc in all the eyes. One week after injection of 1 FU nattokinase, the mild hemorrhages were still observed, but the area gradually reduced.

Discussion

Safer surgical procedures for removing the vitreous in the treatment of vitreoretinal diseases such as proliferative diabetic retinopathy (PVR) and numerous macular diseases are constantly being sought. Among them, enzyme-assisted vitrectomy has been advocated as a useful surgical modality for the treatment of vitreoretinal diseases. Hyaluronidase, which breaks down hyaluronan, facilitates vitreous liquefaction and vitreous hemorrhage absorption; however, it is known that hyaluronidase does not induce PVD.[23,24] In contrast, it has been reported that autologous plasmin is useful in inducing PVD and in facilitating vitreoretinal surgery in clinical cases.[15–18] However, the purification of autologous plasmin requires sterile facilities and trained personnel to perform. Thus, the development of another form has been regarded as important in the treatment of many proliferative vitreoretinal diseases and macular diseases.

In this study, ultrastructural observation with SEM revealed a loss of vitreous fibers on the retinal surface, suggesting the occurrence of PVD induced by nattokinase. Also, concerning the safety of the nattokinase injection, the histology of the retina 30 minutes after the administration of several doses of nattokinase showed no significant damage. In addition, ERGs after the injection of amounts of nattokinase sufficient to induce PVD revealed no critical reductions in the a- and b-wave amplitudes. These results suggest that using an adequate dose of nattokinase as a pharmacologic adjunct to pharmacologic vitreolysis and/or enzyme-assisted vitrectomy in patients with vitreoretinal disorders is very promising.

The mass purification of this *B. subtilis* (natto)-derived enzyme is achieved with an easy and convenient protocol in comparison with plasmin. The clinical application of this enzyme will enable us to perform pharmacologic vitreolysis and/or enzyme-assisted vitrectomy even in medical centers without the facilities or trained personnel to purify autologous plasmin, and in patients requiring urgent surgery. In addition, unlike with autologous plasmin, we can obtain uniform enzymatic activity by the use of purified nattokinase among individual cases. These advantages make nattokinase a reasonable alternative in all medical centers for performing safer and less invasive treatment for vitreoretinal disorders.

Nattokinase hydrolyzes collagen fiber, which is a matrix component of the vitreous, indicating effectiveness in liquefying the vitreous gel when injected into the vitreous cavity. In the present study, SEM showed smooth retinal surfaces without vitreous fibers, suggesting strong and broad cleavage of some materials in the interface between the retina and vitreous by nattokinase. Regarding the mechanisms of PVD induction, our previous study suggested that the activation of endogenous matrix metalloproteinase-2 by exogenous plasmin is associated with the induction of PVD.[25] Despite having considerably different amino acid sequences, nattokinase and plasmin share some common features: both are serine proteases and both have a high affinity for fibrin. Nattokinase not only has potent fibrinolytic activity but also enhances plasminogen activators and inactivates a plasminogen activator inhibitor.[20–22] Therefore, regarding the PVD-inducing mechanism, we think that nattokinase may have two major effects: one is the direct effect of liquefying the vitreous gel by its proteolytic activity and the other is the indirect effect of increasing the plasmin activity that induces the vitreoretinal dehiscence. In further studies, the details of the mechanisms related to nattokinase's PVD-inducing effects should be revealed. Concerning the therapeutic dose of nattokinase from this study, we think that 0.1 FU is adequate for pharmacologic vitreolysis. After administration of 1 FU nattokinase, the experimental eyes showed preretinal hemorrhage and histologic alteration. Although we did not determine the relationship between these findings, it may not be a direct toxic effect on ocular tissues, but rather the result of sudden separation of the posterior vitreous cortex from the retina that was induced by the higher dose. Further study of the optimal concentration of nattokinase and the mechanism of its adverse effects should be conducted. Further study is also necessary to determine an adequate exposure time to this enzyme and any adverse effects after an injection of nattokinase combined with a mechanical vitrectomy.

In conclusion, our findings suggest that nattokinase may be a useful pharmacologic adjunct in vitreous surgery.

References

1. Sebag J. Macromolecular structure of vitreous. *Prog Polym Sci.* 1998;23:415–446.
2. Sebag J. Pharmacologic vitreolysis. *Retina.* 1998;18:1–3.
3. Trese MT. Enzymatic vitreous surgery. *Semin Ophthalmol.* 2000; 15:116–121.
4. Tanaka M, Qui H. Pharmacological vitrectomy. *Semin Ophthalmol.* 2000;15:51–61.
5. Sebag J. Is pharmacologic vitreolysis brewing? *Retina.* 2002;22: 1–3.
6. Gottlieb JL, Antoszyk AN, Hatchell DL, Saloupis P. The safety of intravitreal hyaluronidase: a clinical and histologic study. *Invest Ophthalmol Vis Sci.* 1990;31:2345–2352.
7. Harooni M, McMillan T, Refojo M. Efficacy and safety of enzymatic posterior vitreous detachment by intravitreal injection of hyaluronidase. *Retina.* 1998;18:16–22.
8. Verstraeten TC, Chapman C, Hartzer M, et al. Pharmacologic induction of posterior vitreous detachment in the rabbit. *Arch Ophthalmol.* 1993;111:849–854.
9. Hikichi T, Yanagiya N, Kado M, et al. Posterior vitreous detachment induced by injection of plasmin and sulfur hexafluoride in the rabbit vitreous. *Retina.* 1999;19:55–58.
10. Gandorfer A, Putz E, Welge-Lussen U, et al. Ultrastructure of the vitreoretinal interface following plasmin assisted vitrectomy. *Br J Ophthalmol.* 2001;85:6–10.
11. Kim NJ, Yu HG, Yu YS, Chung H. Long-term effect of plasmin on the vitreolysis in rabbit eyes. *Korean J Ophthalmol.* 2004;18:35–40.
12. Wang F, Wang Z, Sun X, et al. Safety and efficacy of dispase and plasmin in pharmacologic vitreolysis. *Invest Ophthalmol Vis Sci.* 2004;45:3286–3290.
13. Gandorfer A, Priglinger S, Schebitz K, et al. Vitreoretinal morphology of plasmin-treated human eyes. *Am J Ophthalmol.* 2002;133: 156–159.
14. Li X, Shi X, Fan J. Posterior vitreous detachment with plasmin in the isolated human eye. *Graefes Arch Clin Exp Ophthalmol.* 2002; 240:56–62.
15. Margherio AR, Margherio RR, Hartzer M, et al. Plasmin enzyme-assisted vitrectomy in traumatic pediatric macular holes. *Ophthalmology.* 1998;105:1617–1620.
16. Trese MT, Williams GA, Hartzer MK. A new approach to stage 3 macular holes. *Ophthalmology.* 2000;107:1607–1611.
17. Williams JG, Trese MT, Williams GA, Hartzer MK. Autologous plasmin enzyme in the surgical management of diabetic retinopathy. *Ophthalmology* 2001;108:1902–1905; discussion 1905–1906.
18. Azzolini C, D'Angelo A, Maestranzi G, et al. Intrasurgical plasmin enzyme in diabetic macular edema. *Am J Ophthalmol.* 2004;138: 560–566.

19. Nakamura T, Yamagata Y, Ichishima E. Nucleotide sequence of the subtilisin NAT gene, aprN, of Bacillus subtilis (natto). *Biosci Biotechnol Biochem*. 1992;56:1869-1871.
20. Sumi H, Hamada H, Tsushima H, et al. A novel fibrinolytic enzyme (nattokinase) in the vegetable cheese Natto; a typical and popular soybean food in the Japanese diet. *Experientia*. 1987;43:1110-1111.
21. Sumi H, Hamada H, Nakanishi K, Hiratani H. Enhancement of the fibrinolytic activity in plasma by oral administration of nattokinase. *Acta Haematol*. 1990;84:139-143.
22. Urano T, Ihara H, Umemura K, et al. The profibrinolytic enzyme subtilisin NAT purified from Bacillus subtilis cleaves and inactivates plasminogen activator inhibitor type 1. *J Biol Chem*. 2001; 276:24690-24696.
23. Hikichi T, Kado M, Yoshida A. Intravitreal injection of hyaluronidase cannot induce posterior vitreous detachment in the rabbit. *Retina*. 2000;20:195-198.
24. Wang ZL, Zhang X, Xu X, et al. PVD following plasmin but not hyaluronidase: implications for combination pharmacologic vitreolysis therapy. *Retina*. 2005;25:38-43.
25. Takano A, Hirata A, Inomata Y, et al. Intravitreal plasmin injection activates endogenous matrix metalloproteinase-2 in rabbit and human vitreous. *Am J Ophthalmol*. 2005;140:654-660.

Journal of Neurochemistry, 2006, **98**, 372–385 doi:10.1111/j.1471-4159.2006.03871.x

Thioredoxin inhibits NMDA-induced neurotoxicity in the rat retina

Yasuya Inomata,*† Hajime Nakamura,‡ Masaki Tanito,§ Akie Teratani,‡ Takahiro Kawaji,† Norihiko Kondo,* Junji Yodoi* and Hidenobu Tanihara†

**Department of Biological Responses, Institute for Virus Research, Kyoto University, Kyoto, Japan*

†Departments of Ophthalmology and Visual Science, Kumamoto University Graduate School of Medical Sciences, Kumamoto, Japan

‡Thioredoxin Project, Department of Experimental Therapeutics, Translational Research Center, Kyoto University Hospital, Kyoto, Japan

§Department of Ophthalmology, University of Oklahoma Health Sciences Center, Oklahoma, USA

Abstract

Thioredoxin (TRX) plays a variety of redox-related roles in organisms. To investigate its function as an endogenous redox regulator in NMDA-induced retinal neurotoxicity, we injected NMDA with TRX, mutant TRX or saline into the vitreous cavity of rat eyes. Retinal ganglion cells were rescued by TRX, compared with saline, when evaluated by retrograde labeling analysis at 7 days after NMDA injection. TRX, but not its mutant form, prevented NMDA-induced apoptosis in the retina, as measured by terminal deoxynucleotidyl transferase-mediated UTP nick-end labeling. The induction of caspase 3 and 9, but not caspase 8, by NMDA was significantly lower in TRX-treated eyes than in saline-treated eyes. NMDA-induced activation of the MAPKs, p38 kinase and c-Jun N-terminal kinase after 6 h and of the MAPK kinases (MKKs) MKK3/6 and MKK4 after 3 h was markedly suppressed in retinal ganglion cells by TRX but not by the mutant form. NMDA-induced increases in protein carbonylation, nitrosylation and lipid peroxidation were also suppressed in TRX-treated eyes. We concluded that the intravitreous injection of TRX effectively attenuated NMDA-induced retinal cell damage and that suppression of oxidative stress and inhibition of apoptotic signaling pathways were involved in this neuroprotection.

Keywords: apoptosis, mitogen-activated protein kinases, NMDA, oxidative stress, retinal ganglion cells, thioredoxin.

J. Neurochem. (2006) **98**, 372–385.

Apoptotic cell death is a feature of various eye diseases, including retinal ischemia (Levin and Louhab 1996; Rosenbaum *et al.* 1998) and glaucoma (Levin and Louhab 1996). Neurotoxicity induced by excitatory amino acids, such as glutamate, is a major mechanism underlying retinal damage in such diseases (Schwarcz and Coyle 1977; Sucher *et al.* 1997). This excitotoxicity has been shown to be mediated by over-stimulation of both NMDA-type and non-NMDA-type glutamate receptors in the retina (Lam *et al.* 1999), with NMDA-type receptors being most strongly implicated in neuronal cell death (Bonfoco *et al.* 1995). A number of cells in the eye, including retinal ganglion cells (RGCs) and amacrine cells, express this receptor (Brandstatter *et al.* 1994). Indeed, administration of NMDA to rodent eyes hyperstimulates glutamate receptors and induces retinal damage, with free radicals, including reactive oxygen species, playing an important role in this process (Siliprandi *et al.* 1992; El-Remessy *et al.* 2003). This animal model has been widely used to investigate the mechanism of retinal neuronal cell death and the role of apoptosis, and to evaluate neuroprotective factors and biological drugs (Inomata *et al.* 2003a,b; Hartwick *et al.* 2004; Wehrwein *et al.* 2004). The MAPK superfamily, which consists of c-Jun N-terminal kinase (JNK), p38 kinase (p38) and extracellular signal-regulated kinase, is stimulated by various cellular stresses. Recently, roles for the p38 and JNK signal pathways were

Received November 22, 2005; revised manuscript received February 13, 2006; accepted February 21, 2006.

Address correspondence and reprint requests to Hajime Nakamura, Thioredoxin Project, Department of Experimental Therapeutics, Translational Research Center, Kyoto University Hospital, 54 Shogoin-Kawaharacho, Sakyo, Kyoto, 606-8507, Japan.
E-mail: hnakamur@kuhp.kyoto-u.ac.jp

Abbreviations used: DM, double-mutant; GCL, ganglion cell layer; INL, inner nuclear layer; JNK, c-Jun N-terminal kinase; MDA, malondialdehyde; MKK, MAPK kinase; p, phospho; p38, p38 kinase; RGC, retinal ganglion cell; rh, recombinant human; TRX, thioredoxin; TUNEL, terminal deoxynucleotidyl transferase-mediated UTP nick-end labeling; WT, wild-type.

reported in NMDA-induced RGC apoptosis (Manabe and Lipton 2003; Munemasa *et al.* 2005).

Thioredoxin (TRX), which is a ubiquitous 12-kDa multifunctional protein, plays a variety of redox-related roles in organisms ranging from *Escherichia coli* to humans (Holmgren 1985). Human TRX was originally cloned as a soluble factor released from human T-cell leukemia virus-I-transformed T cells (Tagaya *et al.* 1989; Yodoi and Uchiyama 1992). It has two redox-active cysteine residues in its active center, Cys^{32}-Gly-Pro-Cys^{35}, which undergo reversible oxidation–reduction reactions catalysed by an NADPH-dependent enzyme, TRX reductase (Holmgren 1985). TRX is induced by various oxidant stresses, including viral infection and ischemia/reperfusion, and secreted from cells (Nakamura *et al.* 1997; Kondo *et al.* 2004). TRX plays a crucial role in the redox regulation of transcriptional factors such as nuclear factor-kappa B and shows antioxidative, anti-inflammatory and antiapoptotic effects (Nakamura *et al.* 1997, 2001). Overexpression or administration of TRX protects against neuronal damage associated with oxidative stress (Takagi *et al.* 1999; Bai *et al.* 2003; Hattori *et al.* 2004). Moreover, TRX effectively inhibits retinal damage including light-induced photic injury and ischemia/reperfusion injury (Shibuki *et al.* 1998; Tanito *et al.* 2002b,c). Current information suggests that TRX regulates apoptosis through a wide variety of mechanisms, including scavenging reactive oxygen species, regulating cytochrome *c* release from mitochondria, and regulating MAPKs and their upstream regulators (Masutani *et al.* 2005).

The purpose of the current study was to investigate the potential neuroprotective effects of TRX in NMDA-induced retinal damage *in vivo*. To further elucidate the mechanisms involved, we assessed terminal deoxynucleotidyl transferase-mediated UTP nick-end labeling (TUNEL), the activity of caspase 3, 8 and 9, the phosphorylation of the MAPKs p38 and JNK and the MAPK kinases (MKKs) MKK3/6 and MKK4, and the oxidation status of proteins in terms of their carbonylation, nitrosylation and lipid peroxidation in NMDA-treated retinas.

Materials and methods

Antibodies

Rabbit polyclonal antibodies against JNK, phospho (p)-JNK, MKK3/MKK6, p-MKK3/MKK6, MKK4 and p-MKK4 were purchased from Cell Signaling Technology (Beverly, MA, USA). Rabbit polyclonal antibodies against p38 and p-p38 were purchased from Sigma Chemical Co. (St Louis, MO, USA).

Animals

Male 9-week-old Wistar rats weighing 180–200 g were housed at 25°C under a 12-h light–dark cycle, and given water and food *ad libitum*. All studies were conducted in accordance with the Association for Research in Vision and Ophthalmology Statement on the Use of Animals in Ophthalmic and Vision Research.

NMDA-induced retinal damage

Intravitreal injection of NMDA (Sigma Chemical Co.) was performed as previously reported (Inomata *et al.* 2003a,b). Briefly, rats were anesthetized by injecting 50 mg/kg pentobarbital intraperitoneally, the right pupil was dilated with phenylephrine hydrochloride and tropicamide drops, and 20 nmol of NMDA was injected into the vitreous cavity. Injections were performed under a microscope using a 33-gauge needle connected to a microsyringe and the needle was inserted approximately 1 mm behind the corneal limbus.

Thioredoxin treatment

Recombinant human (rh) TRX was provided by Ajinomoto (Kawasaki, Japan; Mitsui *et al.* 1992). Preparation of 6× histidine-tagged wild-type (WT) TRX and double-mutant (DM) TRX, in which the two cysteines at positions 32 and 35 were replaced with serine, was as described previously (Liu *et al.* 2004). A 100-μg sample of rhTRX, WT-TRX, DM-TRX or saline as a vehicle control, mixed with NMDA in a total volume of 3 μL, was injected into the vitreous cavity.

Recombinant human TRX was labeled using an Alexa Fluor 594 Labelling Kit (Molecular Probes, Eugene, OR, USA), according to the manufacturer's protocol, and was used to assess the distribution in the retina. Aliquots (10 μg) were injected in a total volume of 2 μL into the vitreous cavity. The eyes were enucleated 1, 6, 12 or 24 h later, fixed in 4% paraformaldehyde and embedded in optical cutting temperature compound. Sections (10 μm thick) were cut with a cryostat and examined by fluorescence microscopy.

Retrograde labeling of retinal ganglion cells

At 4 days after the NMDA injection, retrograde labeling of RGCs was performed as described previously (Inomata *et al.* 2003a,b). Briefly, rats were anesthetized, their heads immobilized and Fluoro-Gold (Fluorochrome, Englewood, CO, USA) was microinjected bilaterally into the superior colliculi. After 3 days (7 days after the NMDA injection), the eyes were enucleated and fixed in 4% paraformaldehyde for 1 h. The retinas were divided by six radial cuts, removed from the sclera and mounted on slides. The numbers of Fluoro-Gold-labeled RGCs were counted in the locations described previously (Inomata *et al.* 2003a,b). Briefly, labeled RGCs were counted in two fields in the central area (1 mm from the optic disc) and two fields in the peripheral area (4 mm from the optic disc).

Terminal deoxynucleotidyl transferase-mediated UTP nick-end labeling

Rats were killed with an overdose of sodium pentobarbital 24 h after the NMDA injection, and their eyes were immediately enucleated and fixed in 4% paraformaldehyde in phosphate-buffered saline. TUNEL was performed using a fluorescent apoptosis-detection system (Promega, Madison, WI, USA) on 5-μm-thick paraffin-embedded sections. TUNEL-positive cells were counted in the locations described previously (Inomata *et al.* 2003a,b), i.e. the ganglion cell layer (GCL) and the inner nuclear layer (INL) 1.0–1.5 mm from the optic disc.

Caspase assays

Caspase protease activities were measured as reported previously, with slight modifications (Ueda *et al.* 1998). Caspase 3, 8 and 9 cleaved the fluorogenic peptides *N*-acetyl-Asp-Glu-Val-Asp-7-amino-4-trifluoromethyl coumarin, *N*-acetyl-Ile-Glu-Thr-Asp-7-amino-4-trifluoromethyl coumarin and *N*-acetyl-Leu-Glu-His-Asp-7-amino-4-trifluoromethyl coumarin, respectively. Briefly, the retinas were removed after NMDA injection, immediately homogenized in lysis buffer containing 50 mM Tris-HCl, 1 mM EDTA and 10 mM EGTA, and centrifuged at 20 000 *g* for 15 min. The supernatants were incubated with 50 μM fluorogenic peptide at 37°C. Release of 7-amino-4-trifluoromethyl coumarin was monitored using a fluorescence microplate reader (Gemini EM; Molecular Devices, Sunnyvale, CA, USA) at excitation and emission wavelengths of 380 and 460 nm, respectively. For caspase 3 and 8, 1 U was defined as the release of 0.13 pmol 7-amino-4-trifluoromethyl coumarin/min/mg retinal protein. For caspase 9, 1 U was defined as the release of 0.12 pmol 7-amino-4-trifluoromethyl coumarin/min/mg retinal protein (Ueda *et al.* 1998).

Western blot analysis

Eyes were enucleated at various times after NMDA injection. The retinas were then removed and homogenized in cell lysis buffer (Kinase Assay Kit: Cell Signaling Technology). The lysates were centrifuged at 20 000 *g* for 15 min at 4°C. Protein concentrations in the supernatants were determined using a DC Protein Assay Kit (Bio-Rad Laboratories, Hercules, CA, USA). Equal amounts of protein (20 μg/lane) were separated on 10% sodium dodecyl sulfate–polyacrylamide gels and then electrophoretically transferred to polyvinylidene difluoride membranes. After blocking in Tris-buffered saline containing 0.1% Tween 20 and 5% bovine serum albumin, the membranes were incubated overnight at 4°C with 1 : 1000 dilutions of primary antibodies against p38, p-p38, JNK, p-JNK, MKK3, p-MKK3/MKK6, MKK4 or p-MKK4, followed by a peroxidase-linked second antibody (Amersham Pharmacia, Buckinghamshire, UK; 1 : 5000). Chemiluminescence was detected with an enhanced chemiluminescence western blot detection kit (Amersham Pharmacia).

Immunohistochemistry

At 6 h after NMDA injection, the eyes were enucleated, fixed in 4% paraformaldehyde in phosphate-buffered saline and soaked in a cryoprotective 20% sucrose solution overnight at 4°C before being frozen in optical cutting temperature compound (Tissue-Tek; Sakura Finetechnical Co. Ltd, Tokyo, Japan). Cryostat sections (10 μm thick) were mounted on glass slides coated with poly-L-lysine, incubated with Protein Block Solution (DAKO, Glostrup, Denmark) and then incubated overnight at 4°C with either anti-p-p38 antibody (1 : 100) or anti-p-JNK antibody (1 : 100). The sections were washed three times and incubated with Alexa Fluor 488-labeled anti-rabbit IgG (Molecular Probes; 1 : 200) at 25°C for 1 h. They were then washed three times, exposed to one drop of Vectashield Mounting Medium with 4′,6-diamidino-2-phenylindole (Vector Laboratories, Burlingame, CA, USA) to stain the nuclei and examined by fluorescence microscopy.

Protein carbonylation assay

The level of protein oxidation induced by NMDA was measured using an OxyBlot kit (Chemicon, Temecula, CA, USA), which is a sensitive immunodetection method for carbonyl groups, as described previously (Tanito *et al.* 2002a). Retinas were removed 18 h after NMDA injection and homogenized with ice-cold phosphate-buffered saline (20 mM, pH 7.4). The homogenates were centrifuged at 20 000 *g* for 15 min and the supernatants were used to prepare 2,4-dinitrophenyl-hydrazone derivatives, according to the manufacturer's protocol. The samples were separated on 12% sodium dodecyl sulfate–polyacrylamide gels and transferred to polyvinylidene difluoride membranes (Millipore, Bedford, MA, USA). After blocking, the membrane was incubated initially with a primary antibody specific for 2,4-dinitrophenyl and then with a peroxidase-linked secondary antibody. Chemiluminescence was detected with an enhanced chemiluminescence western blot detection kit (Amersham Pharmacia). An image scanner was used to scan each lane and the intensities of protein bands were analysed by using NIH IMAGE 1.63 software according to the software tutorial.

Nitrotyrosine enzyme immunoassay

The formation of peroxynitrite ($ONOO^-$), which is short-lived at physiological pH but easily nitrosylates tyrosine residues, was assessed in retinas by measuring the concentration of nitrotyrosine using an enzyme immunoassay kit (Cell Sciences, Norwood, MA, USA), according to the manufacturer's protocol. Retinal samples were prepared as for the protein carbonylation assay and assays were performed in duplicate.

Lipid peroxidation assay

We determined lipid peroxidation induced by NMDA by measuring malondialdehyde (MDA) in retinal samples with a Bioxytech LPO-586 assay kit (Oxis International, Portland, OR, USA), according to the manufacturer's protocol. Samples (100 μL), adjusted to contain 100 μg retinal protein, were prepared from retinas as for the protein carbonylation assay. *N*-methyl-2-phenylindole was used as the chromogen and measurements were made at an absorbance of 586 nm. We used 1,1,3,3-tetramethoxypropane as an external standard and the level of lipid peroxide was expressed as pmol MDA/mg protein.

Statistical analysis

The data presented as bar graphs show the means ± SD of at least four independent experiments. The differences between groups were evaluated by one-way ANOVA followed by Scheffe's post-hoc test for multiple comparisons. p values < 0.05 were considered statistically significant.

Results

Distribution of thioredoxin in the retina after intravitreous injection

To examine the distribution of TRX in the retina after injection, 10 μg Alexa-labeled rhTRX was injected into the vitreous cavity. After 1 h, Alexa-labeled rhTRX was detected in all retinal layers, including the retinal pigment epithelium layer (Fig. 1). The distribution had not changed significantly 12 h after injection. At 24 h, labeling increased in the rod inner segment and the rod outer segment, and decreased in the inner plexiform layer and the outer plexiform layer.

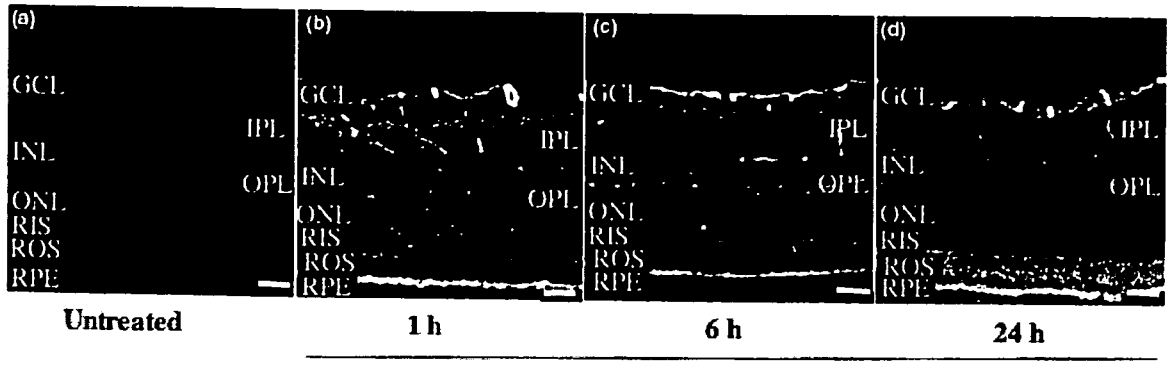

Fig. 1 Distribution of thioredoxin (TRX) in retinal tissue. Photographs of representative retinal sections were examined by fluorescence microscopy for labeling due to Alexa 594-TRX. Sections were from untreated eyes (a) or eyes treated with 10 μg recombinant human (rh)TRX injected into the vitreous cavity 1 h (b), 6 h (c) or 24 h (d) previously. Alexa labeling was detected in all retinal layers, including the retinal pigment epithelium (RPE) layer, at 1 h and up to 24 h after injection. Scale bars, 50 μm. GCL, ganglion cell layer; INL, inner nuclear layer; IPL, inner plexiform layer; ONL, outer nuclear layer; OPL, outer plexiform layer; RIS, rod inner segment; ROS, rod outer segment.

Neuroprotective effects of thioredoxin on retinal ganglion cells using retrograde labeling

To investigate whether exogenous TRX could protect RGCs from NMDA-induced cell death, we carried out retrograde labeling experiments with Fluoro-Gold (Fig. 2). Compared with a density of 1006 ± 55 RGCs/mm^2 in control eyes treated with saline alone, the density of RGCs was significantly lower in eyes examined 7 days after NMDA injection (135 ± 15 cells/mm^2; $p < 0.001$). However, in eyes treated with TRX, the effect of NMDA on the density of RGCs after 7 days was significantly suppressed, with 210 ± 19 cells/mm^2 ($p < 0.05$) and 570 ± 38 cells/mm^2 ($p < 0.05$) in eyes treated with 100 or 400 μg rhTRX, respectively (Fig. 2d).

Effects of thioredoxin on NMDA-induced apoptosis

We investigated whether TRX inhibited NMDA-induced apoptosis by assessing the numbers of TUNEL-positive cells 24 h after NMDA injection in retinal sections. As shown previously, TUNEL-positive cells were present in the INL and GCL after 24 h (Fig. 3a; Inomata *et al.* 2003a,b). However, in eyes treated with rhTRX or WT-TRX, the total numbers of TUNEL-positive cells in the retinal sections were significantly lower compared with vehicle-treated ($p < 0.001$) and DM-TRX-treated eyes ($p = 0.044$ for rhTRX and 0.002 for WT-TRX; Fig. 3e). Moreover, when the numbers of TUNEL-positive cells in specific parts of the retina were counted, significant differences were found in both the GCL and INL between eyes treated with rhTRX and WT-TRX compared with vehicle ($p < 0.001$). The differences in the numbers of apoptotic cells were also significant when eyes treated with DM-TRX were compared with eyes treated with rhTRX in the GCL ($p = 0.003$) or INL ($p = 0.049$), or compared with eyes treated with WT-TRX in the GCL ($p = 0.006$) or INL ($p = 0.002$; Figs 3f and g). These results indicated that the redox-active site sequence Cys-Gly-Pro-Cys in TRX might play an important role in its antiapoptotic effect.

Inhibition of the mitochondrial apoptotic pathway by thioredoxin

As caspase activity is generally required for apoptosis, we assessed the effect of TRX on caspases induced by NMDA. We measured the induction of these caspases at 6, 12, 18 and 24 h after NMDA injection, and the induction of caspase 3 peaked at 18 h and caspase 9 and 8 peaked at 12 h, respectively (data not shown). In eyes treated with NMDA and vehicle, caspase 3 was induced in the retina after 18 h (73.3 ± 23.8 U) but this activity was significantly inhibited in TRX-treated retinas (38.8 ± 21.8 U; $p = 0.035$; Fig. 4c). NMDA also induced caspase 9 in the retina after 12 h (18.5 ± 5.3 U) but this activity was significantly inhibited in TRX-treated eyes (11.4 ± 4.5 U; $p = 0.045$; Fig. 4a). By contrast, NMDA failed to induce caspase 8 (Fig. 4b) and we observed no significant differences in caspase 8 activity between vehicle and rhTRX treatment after NMDA administration. These results indicated that NMDA-induced apoptosis was mediated by the mitochondrial pathway (Cao *et al.* 2001) and that TRX exerted an antiapoptotic effect on this pathway.

Thioredoxin inhibits NMDA-induced phosphorylation of p38 and c-Jun N-terminal kinase

We next asked whether the MAPKs p38 and JNK, which might form part of the upstream signaling cascades in the mitochondrial apoptosis pathway, were involved in the cellular response to NMDA, and whether they were affected

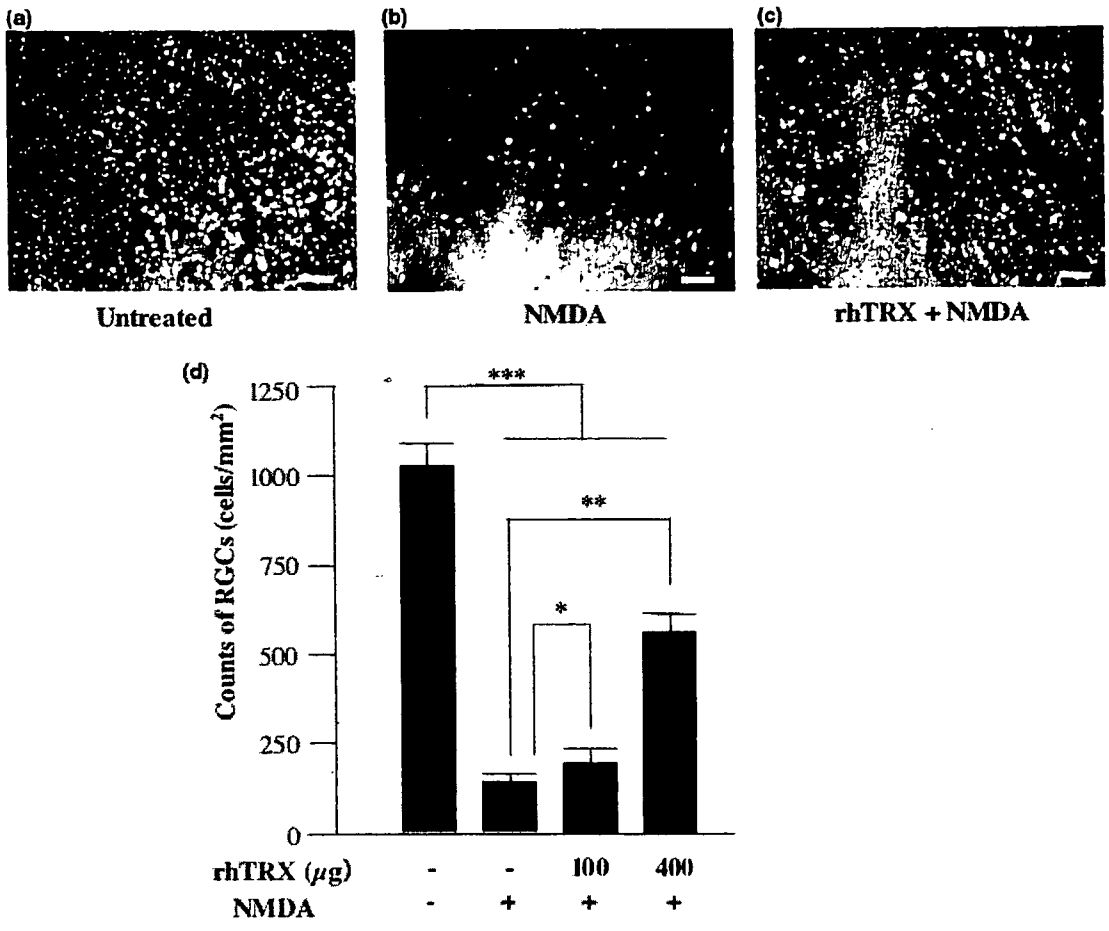

Fig. 2 Density of retinal ganglion cells (RGCs) 7 days after NMDA injection. Fluorescence microscopic photographs of representative retinal sections in untreated (a) and NMDA-treated (b and c) eyes simultaneously injected with vehicle (b) or 100 μg recombinant human thioredoxin (rhTRX) (c). Scale bars, 50 μm. (d) Mean ± SD cell densities are shown as bar graphs ($n = 4$ in each group). The statistical significance of differences between groups was calculated by one-way ANOVA followed by Scheffe's post-hoc test. $^{*}p < 0.05$, $^{**}p < 0.01$ and $^{***}p < 0.001$.

by the administration of TRX. In western blot analysis, the level of p-p38 was shown to gradually increase after NMDA injection, with maximal expression seen after 6 h (Fig. 5a). The level of p-p38 was clearly lower in vehicle-treated eyes than in eyes that were also treated with rhTRX and WT-TRX (Fig. 5b). The expression of p38 did not change after NMDA injection in either sample. No change in p-p38 or p38 was observed in eyes injected with vehicle alone compared with untreated eyes (data not shown). The results of immunohistochemical labeling for p-p38 showed that, at 6 h after NMDA injection, positive cells were present in the GCL and INL in eyes treated with vehicle but the labeling was clearly reduced in rhTRX-treated eyes (Figs 5c–h).

Western blot analysis showed that the levels of both p-JNK-1 and p-JNK-2 gradually increased after NMDA injection, and reached a maximum after 6 h (Fig. 6a). In eyes treated with rhTRX or WT-TRX as well as NMDA, the levels of phosphorylation of both JNK-1 and JNK-2 were clearly lower than those in eyes treated with vehicle or DM-TRX (Fig. 6b). The expression of JNK did not change after NMDA injection. No changes in p-JNK or JNK were observed in eyes injected with vehicle alone compared with untreated eyes (data not shown). The results of immunohistochemical labeling for p-JNK (Figs 6c–h) showed that, at 6 h after NMDA injection, positive cells were observed in the GCL in vehicle-treated eyes and the labeling was clearly inhibited in eyes that were also treated with rhTRX.

Inhibition of NMDA-induced phosphorylation of MAPK kinases by thioredoxin

We further investigated the phosphorylation of the kinases upstream of MAPKs (i.e. MKK3/MKK6, which activates p38, and MKK4, which activates JNK) by western blot analysis. The levels of p-MKK3/MKK6 (Fig. 7a) and

